Title
Islet Amyloid Polypeptide Membrane Interactions: Effects of Membrane Composition

Journal
Biochemistry, 56(2)

ISSN
0006-2960

Authors
Zhang, Xiaoxue
St. Clair, Johnna R
London, Erwin
et al.

Publication Date
2017-01-17

DOI
10.1021/acs.biochem.6b01016

Peer reviewed

HHS Public Access

Author manuscript

Biochemistry. Author manuscript; available in PMC 2018 January 17.

Published in final edited form as:

Biochemistry. 2017 January 17; 56(2): 376–390. doi:10.1021/acs.biochem.6b01016.

Islet Amyloid Polypeptide Membrane Interactions: Effects of Membrane Composition

Xiaoxue Zhang[1], **Johnna R. St. Clair**[2], **Erwin London**[1,2,*], and **Daniel P. Raleigh**[1,3,*]

[1]Department of Chemistry, Stony Brook University, Stony Brook, NY, 11794-3400

[2]Department of Biochemistry and Cell Biology, Stony Brook University, Stony Brook, NY, 11794-5215

[3]Graduate Program in Biochemistry and Structural Biology, Stony Brook University, Stony Brook, NY, 11794-5215

Abstract

Amyloid formation by islet amyloid polypeptide (IAPP) contributes to β-cell dysfunction in type-2 diabetes. Perturbation of the β-cell membrane may contribute to IAPP induced toxicity. We examine the effects of lipid composition, salt and buffer on IAPP amyloid formation and on the ability of IAPP to induce leakage of model membranes. Even low levels of anionic lipids promote amyloid formation and membrane permeabilization. Increasing the percentage of the anionic lipids, POPS or DOPG, enhances the rate of amyloid formation and increases membrane permeabilization. The choice of zwitterionic lipid has no noticeable effect on membrane catalyzed amyloid formation, but in most cases affects leakage, which tends to decrease in the order DOPC>POPC>sphingomyelin. Uncharged lipids that increase membrane order reduce the ability of IAPP to induce leakage. Leakage is due predominately to pore formation rather than complete disruption of the vesicles under the conditions of these studies. Cholesterol at or below physiological levels significantly reduces the rate of vesicle catalyzed IAPP amyloid formation and decreases susceptibility to IAPP induced leakage. The effects of cholesterol on amyloid formation are masked by 25 mole percent POPS. Overall, there is a strong inverse correlation between the time to form amyloid and the extent of vesicle leakage. NaCl reduces the rate of membrane catalyzed amyloid formation by anionic vesicles, but accelerates amyloid formation in solution. The implications for IAPP membrane interactions are discussed, as is the possibility that loss of phosphatidylserine asymmetry enhances IAPP amyloid formation and membrane damage *in vivo* via a positive feedback loop.

[*]**Corresponding Authors** D.P.R: daniel.raleigh@stonybrook.edu, phone: (631) 632-9547; Fax: (631) 632-7960. E.L: erwin.london@stonybrook.edu, phone, (631) 632-8564.

ASSOCIATED CONTENT

Supporting Information: Ten figures showing the effect of different vesicle compositions on the time course of amyloid formation by hIAPP and the time course of hIAPP induced membrane damage, additional figures showing the concentration dependence of carboxyfluorescein fluorescence, the results of FRET studies of vesicle integrity, LUV peptide binding studies, and additional TEM images, as well as one table containing data on effective diameters of LUVs. This material is available free of charge on the ACS Publications website.

Author Contributions

X.Z. designed and conducted experiments and analyzed data. J.R.S.C. conducted experiments. D.P.R. and E.L. designed, directed and supervised the project. D.P.R., E.L. and X.Z. wrote the manuscript.

The authors declare no competing financial interest.

Abstract

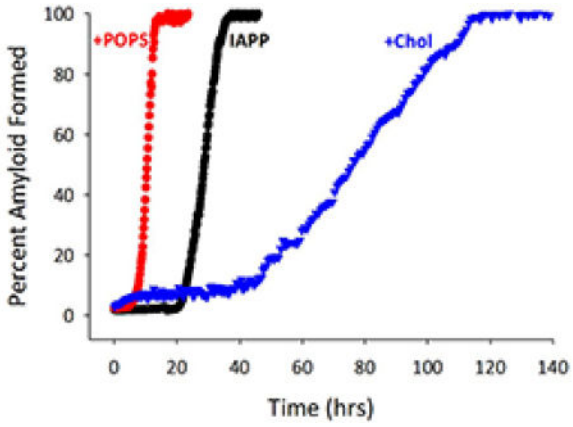

Keywords

Amyloid; Amylin; Islet Amyloid Polypeptide; Peptide Membrane Interactions; Type-2 Diabetes

INTRODUCTION

Islet amyloid polypeptide (IAPP, amylin) is a 37 residue neuropancreatic polypeptide hormone that is co-secreted from the insulin producing β-cells in response to stimuli that lead to insulin release [1]. Human IAPP (hIAPP) plays an adaptive role in metabolism, but converts into insoluble amyloid fibrils in the islets of Langerhans in type-2 diabetes (T2D) [2–17]. β-cell dysfunction and the loss of β-cell mass are key components of T2D, and islet amyloidosis by hIAPP is an important contributor [1–16, 18–27]. Islet amyloid is found in the pancreatic islets of Langerhans in the vast majority of individuals with T2D, and recent studies confirm a correlation between the extent of amyloid deposition and the loss of β-cells [11, 12]. Islet amyloidosis is a major factor in the failure of islet transplants and preventing amyloid deposition prolongs glycemic control [28–30]. Aggregation of IAPP has also been linked to cardiovascular complications downstream of diabetes [31, 32]. A variety of mechanisms of β-cell death have been ascribed to hIAPP including receptor mediated mechanisms, activation of the inflammasome, defects in autophagy and IAPP-induced membrane damage [11, 16, 20, 33–38].

A growing body of work has examined membrane induced aggregation of hIAPP *in vitro*. The vast majority of these studies have used simple binary model membranes containing a super physiological levels of an anionic lipid, typically 1-palmitoyl-2-oleoyl-sn-glycero-3-phospho-L-serine (POPS), 1,2-dioleoyl-sn-glycero-3-phospho-L-serine (DOPS) or 1,2-dioleoyl-sn-glycero-3-phospho-(1'-rac-glycerol) (DOPG), together with a zwitterionic lipid, often 1,2-dioleoyl-sn-glycero-3-phosphocholine (DOPC) or 1-palmitoyl-2-oleoyl-sn-glycero-3-phosphocholine (POPC). IAPP is a cationic polypeptide (Figure-1); its amidated C-terminus and the lack of acidic residues ensure that it is positively charged except at very high pH values. The human polypeptide contains a Lys, an Arg, and a single His, thus the net charge at physiological pH will be between 2 and 4 depending upon the exact pKa of the

N-terminus and His sidechain. hIAPP amyloid formation is accelerated by interactions with membranes that contain a large fraction of anionic lipids and by interactions with negatively charged sulfated glycosaminoglycans [33, 39–56]. IAPP also readily disrupts vesicles that contain significant percentages of anionic lipids [33, 39–50]. The interaction of IAPP with membranes made up of more physiological lipid composition is much less well studied.

The β-cell plasma membrane is very different from most model membrane systems used for *in vitro* biophysical studies. The β-cell membrane contains cholesterol, gangliosides, sphingomyelins, and the level of anionic phospholipids is reported to range from 2.5 to 13.2 mole percent of the total phospholipids [57]. The vast majority of model systems typically contain a much higher percentage of anionic lipids and lack cholesterol and gangliosides, although the effects of cholesterol have been examined in a subset of systems [52, 57–59]. Cholesterol is an important component of membranes; it modulates their biophysical properties and is important for the uptake of hIAPP *in vivo* [58, 60]. The β-cell plasma membrane is also asymmetric, with the anionic lipids predominantly localized to the inner leaflet and the outer leaflet enriched in sphingomyelin. Thus, hIAPP will encounter a very different membrane environment if it interacts with the outer vs the inner leaflet. Extracellular hIAPP will face a membrane that contains a low percentage of anionic lipids, while cytosolic hIAPP will face the cytosolic leaflet with a higher fraction of anionic lipids, but even the cytosolic leaflet of the β-cell membrane contains a modest percentage of anionic lipids. Complicating interpretation of lipid effects, the initiation site of islet amyloid is not understood and there is evidence that both extracellular and intracellular hIAPP oligomers contribute to islet β-cell toxicity [11, 20, 61]. Studies with transgenic mouse models that significantly overexpress hIAPP suggest that islet amyloid may have an intracellular origin, while histological studies show that the amyloid deposits associated with T2D are extracellular. Studies with a transgenic islet model that expresses human levels of hIAPP argue that secretion of hIAPP is required for amyloid formation [11, 62]. Other work shows that toxic hIAPP oligomers can be taken up by cells [58]. Intracellular oligomers in the cytoplasm will face the inner leaflet, but if intracellular oligomers are found in the lumen of an organelle they will face the non-cytosolic (exofacial) leaflet of the membrane, and thus the same lipids as those on the outer surface of the plasma membrane. Thus, it is important to study hIAPP membrane interactions using both mimics of the outer and inner leaflet of the β-cell membrane.

Here we explore the effects of varying the type and amount of anionic lipids, the choice of zwitterionic lipid, the amount of cholesterol and the inclusion of sphingomyelins as well as the effects of varying buffer and salt on IAPP amyloid formation and on IAPP induced membrane leakage. In total 33 different model membrane systems were examined. The studies reveal that standard model membranes behave very differently from membranes which contain physiologically relevant concentrations of cholesterol and anionic lipids and thus they provide guidance to the choice of appropriate model systems for studies of membrane catalyzed hIAPP amyloid formation and hIAPP induced disruption of membranes. The mechanism of IAPP induced membrane leakage is also examined.

MATERIALS AND METHODS

Materials

DOPC, DOPG, 1,2-dioleoyl-sn-glycero-3-phosphoethanolamine-N-(7-nitro-2-1,3-benzoxadiazol-4-yl) (NBD-DOPE), POPC, POPS, 1,2-dioleoyl-sn-glycero-3-phosphoethanolamine-N-(lissamine rhodamine B sulfonyl) (Rho-DOPE), brain sphingomyelin, egg sphingomyelin, cholesterol were obtained from Avanti Polar Lipids. The concentrations of unlabeled lipids were determined by dry weight and that of fluorescent lipids by absorbance using εNBD-DOPE = 21, 000 M^{-1} cm^{-1} at 460 nm in methanol and εRho-DOPE = 95,000 M^{-1} cm^{-1} at 560 nm in methanol. 5(6)-carboxyfluorescein, DMSO, HFIP, thioflavin-T, triton X-100, sucrose and dextrans (FTIC-dextrans) of molecular weight molecular weight 5, 10, 70, 150 kD were obtained from Sigma-Aldrich.

Peptide Synthesis and Purification

Human islet amyloid polypeptide was synthesized on a 0.1 mmol scale using 9-fluoronylmethoxycarbonyl (Fmoc) chemistry with a CEM microwave peptide synthesizer. 5-(4'-fmoc-aminomethyl-3', 5-dimethoxyphenol) valeric acid (Fmoc-Pal-PEG-PS) resin was used to provide an amidated C-terminus. Fmoc-protected pseudoproline dipeptide derivatives were incorporated at positions 9–10, 19–20 and 27–28 [63]. All pseudoprolines, Arg and β-branched residues were double coupled. To reduce racemization, a maximal temperature of 50 °C was used for the His and Cys coupling [64]. Peptides were cleaved from the resin using standard trifluoroacetic acid (TFA) methods. The crude peptides were dissolved in 20% acetic acid (vol/vol) and lyophilized several times. The disulfide bond was formed by dissolving dry peptide in pure dimethyl sulfoxide at room temperature [65]. The peptide was purified using reverse-phase high-performance liquid chromatography with a Proto 300 C18 preparative column (10 mm × 250 mm). A two-buffer system was used. Buffer A consisted of 100% H_2O and 0.045% HCl (vol/vol), and buffer B consisted of 80% acetonitrile, 20% H_2O and 0.045% HCl (vol/vol). HCl was used as the ion-pairing agent instead of TFA, since TFA can affect cell toxicity assays and impact amyloid formation [66]. The molecular weight of the pure product was confirmed using a Bruker AutoFlexII MALDI-TOF/TOF mass spectrometer: human IAPP, expected 3903.3, observed 3902.9. Analytical HPLC was used to check peptide purity before experiments. This is an important control because IAPP can deamidate and this can affect IAPP amyloid formation [67, 68].

Preparation of Peptide Samples

Material from the same synthesis was used in all biophysical studies to ensure comparable conditions for all experiments. Peptide stock solutions were prepared by dissolving pure peptide in 100% HFIP at a concentration of 1.6 mM, filtering through a 0.22 μM Millex low protein binding durapore membrane filter to remove preformed aggregates and stored at 4 °C. Aliquots were lyophilized for 20–24 hours to remove organic solvent and redissolved in buffer at the desired concentration immediately before the experiments started.

Preparation of Large Unilamellar Vesicles

LUVs were prepared from multilamellar vesicles (MLV). MLVs were prepared by dissolving lipids in chloroform in a glass tube at the desired concentration. Mixtures were evaporated with nitrogen gas and were dried in high vacuum for at least 4 hours to completely remove the residual organic solvent. The resulting lipid mixtures were then dispersed in tris buffer (20 mM Tris·HCl, 100 mM NaCl at pH 7.4) and agitated at 55 °C for at least 30 minutes. Samples were cooled to room temperature before use. Large unilamellar vesicles (LUVs) were prepared from MLV by subjecting the MLVs to 7 freeze-thaw cycles and then passing through a 100 nm polycarbonate filter (Avanti Polar Lipids) 11 times to obtain uniform vesicle size. The phospholipid concentration was determined by the method of Stewart [69]. For the membrane leakage experiments, LUVs containing 5(6)-carboxyfluorescein were prepared using the same protocol except that 5(6)-carboxyfluorescein was dissolved in tris buffer (20 mM Tris·HCl, 100 mM NaCl at pH 7.4) at a concentration of 80 mM before lipid hydration. Nonencapsulated 5(6)-carboxyfluorescein was removed from 5(6)-carboxyfluorescein-filled LUVs using a PD-10 desalting column (GE Healthcare Life Sciences) and elution with 20 mM Tris·HCl, 100 mM NaCl buffer, pH 7.4. Dynamic light scattering (DLS) was used to check the effective diameter and polydispersity of each vesicle before use. A fresh vesicle solution was used for each experiment.

Dynamic Light Scattering

Dynamic light scattering experiments were performed on a NanoBrook 90Plus Particle Size Analyzer with a 35 mW red diode laser. The wavelength of irradiation was 640 nm. Membrane samples were prepared to a final concentration of 400 μM with 20 mM Tris·HCl, 100 mM NaCl buffer (pH 7.4). For each sample, three runs were taken at 25 °C with 60 seconds per run. The average diameter (effective diameter) and the distribution width (polydispersity) were calculated using the 90Plus Particle Sizing Software.

Thioflavin-T Fluorescence Assays

Thioflavin-T fluorescence experiments were performed using a Beckman Coulter DTX880 plate reader with excitation and emission wavelengths of 430 nm and 485 nm, respectively. Samples were incubated in 96-well quartz microplate at 25 °C. Samples contained 20 μM peptide in tris buffer (20 mM Tris·HCl, 100 mM NaCl, pH 7.4) with 32 μM Thioflavin-T. This concentration of IAPP was chosen to yield a peptide to lipid ratio of 1:20 since this is typical of values used for studies of hIAPP membrane interactions. Additional experiments were performed to test the effects of varying the buffer. Experiments in the presence of membrane were initiated by adding 400 μM LUVs. Uncertainties in T_{50} were estimated by conducting measurements in triplicate using different solutions of hIAPP.

Membrane Permeability Assays

Leakage experiments were performed using a Beckman Coulter DTX880 plate reader with excitation and emission wavelength filters of 485 nm and 535 nm, respectively. All of the samples were incubated in 96-well quartz microplate at 25 °C. 400 μM 5(6)-carboxyfluorescein-encapsulated LUVs were used and the peptide concentration was 20 μM.

The fluorescence signal of the 5(6)-carboxyfluorescein-encapsulated LUVs was continuously measured during the course of each experiment. The maximum leakage for totally disrupted membranes was measured by adding the detergent Triton X-100 to a final concentration of 0.2% (vol/vol).

The percent change in 5(6)-carboxyfluorescein fluorescence is calculated as:

$$\text{Percent Fluorescence Change} = 100 \times [\mathrm{F(T)} - \mathrm{F_{baseline}}/(\mathrm{F_{max}} - \mathrm{F_{baseline}})$$

Where F(T) is the fluorescence intensity at time T, F_{max} is the fluorescence intensity when all of the vesicles have been disrupted and $F_{baseline}$ is the base line fluorescence is observed before addition of hIAPP. F_{max} was experimentally determined by disrupting the vesicles with Triton X-100. The percent change in fluorescence will equal the percentage change in leakage provided the 5(6)-carboxyfluorescein fluorescence response is linear. Control experiments indicate that this is a reasonable assumption for the studies reported here although when 5(6)-carboxyfluorescein trapping efficiency was high, the response may have been slightly non-linear (Figure-S1, S2). Uncertainties were estimated by repeating the measurements three times using different stock solutions of hIAPP.

Transmission Electron Microscopy

TEM was performed at the Life Science Microscopy Center at Stony Brook University. Aliquots of sample from the thioflavin-T fluorescence experiments were used as TEM samples. Eight microliters of the solution was blotted on a carbon-coated Formvar 300 mesh copper grid for 1 min and then negatively stained for additional 1 min with saturated uranyl acetate.

Sucrose Density Gradient Centrifugation Assays

Sucrose gradient centrifugation was performed using a Beckman L8-55M ultracentrifuge with an SW-60 rotor. Sucrose gradients were prepared by freezing 3.5 ml of 10% (w/w) sucrose at –20 °C in centrifuge tubes overnight and thawing to room temperature. Sucrose concentrations in the fractions were estimated using a refractometer. The highest density was 20 percent sucrose (bottom layer) and the lowest was 5 percent sucrose (top layer). Vesicles contained 2 mole percent NBD-DOPE to allow visualization. Vesicles were incubated with hIAPP until amyloid formation was complete. 500 μl samples were loaded on top of the gradients and samples were then centrifuged for 45 minutes at 37,500 rpm. Vesicles that bind peptide segregate to the bottom layer of the gradient while those that do not float on top of the gradient. The two lipid-containing layers were removed and diluted into 1.2 ml tris buffer. The amount of NBD-DOPE were quantified using a SPEX FluoroLog 3 spectrofluorometer with excitation and emission wavelengths of 465 nm and 534 nm. The slit bandwidths for fluorescence measurements were set to 4.0 nm for both excitation and emission. Background intensities in samples lacking fluorescent probe were negligible (1–2%) and were generally not subtracted from the reported values.

Entrapping FITC dextrans in LUVs

A mixture of 8 mM lipids comprising POPC, POPS, cholesterol, 0.5 mole percent Rho-DOPE and 1.8 mg/ml FITC-dextran were dissolved in 20 mM tris buffer, 100 mM NaCl, pH 7.4. Free FITC-dextran was separated from LUV-trapped dextran by dialysis against tris buffer pH 7.4. Typically, the final lipid concentration was 2–4 mM as determined by Rho-DOPE fluorescence, i.e., by determining the ratio of the fluorescence of Rho-DOPE after sample preparation to that in the vesicles prior to fractionation, assuming that the loss in lipids during dialysis is minimal. The average vesicle diameter, as estimated by DLS, was 106 nm. LUVs were diluted to 400 μM when tested.

FITC dextran leakage assays

FITC-dextran leakage was measured by incubating 400 μM LUVs with 20 μM human IAPP at 25 °C. Samples were incubated for defined time periods and then centrifuged for 50 min in a Beckman L8–55M ultracentrifuge with an SW-60 rotor at 37,500 rpm, 25 °C. After centrifugation, the supernatant containing leaked FITC-dextran was removed, and pellets containing the LUVs were resuspended in tris buffer at pH 7.4. Rho-DOPE and either FITC fluorescence was measured for both the supernatant and the pellet. The efficiency of vesicle pelleting was generally about 60–70% for vesicles without peptide and 70–80% for vesicles with hIAPP. Calculated values were corrected for incomplete pelleting of vesicles using established methods[70].

Forster Resonance Energy Transfer (FRET) Measurements of Lipid Exchange and Vesicle Solubilization

A donor-acceptor pair of NBD-DOPE/Rho-DOPE was used. Fluorescence was measured using an Applied Phototechnology fluorescence spectrophotometer with an excitation wavelength of 465 nm and an emission wavelength of 534 nm. For FRET in labeled vesicles, F samples had a mixture of unlabeled lipid, lipid labeled with NBD, and lipid labeled with rhodamine, while Fo samples had a mixture of unlabeled lipid and lipid labeled with NBD. Background for F samples contained unlabeled lipid with same amount of acceptor as in the F samples. Background samples for Fo contained pure unlabeled lipid. The mole percent of labeled lipids in the “F sample” labeled vesicles was 0.5 mole percent NBD-DOPE and 1.0 mole percent Rho-DOPE. For FRET experiments, LUVs were incubated in the presence and absence of hIAPP at a lipid to peptide ratio of 20:1 (20 μM hIAPP). Aliquots of each samples were diluted by a factor of 4 using tris buffer before fluorescence measurements. Uncertainties were estimated by conducting three independent experiments using samples from different solutions of hIAPP.

RESULTS

The primary sequence of hIAPP is displayed in Figure-1. The polypeptide contains an amidated C-terminus, a disulfide bond between residue 2 and 7 and has no acidic residues. Positively charged residues include Lys-1, Arg-11 and potentially His-18 depending upon its pKa. We first describe studies designed to test the ability of different model membrane systems to catalyze hIAPP amyloid formation using large unilamellar vesicles (LUVs) composed of different lipids with and without cholesterol. We then probe the ability of

hIAPP to permeabilize these model membranes using dye leakage assays and examined the mechanism of leakage using FRET assays and size dependent leakage assays.

Anionic lipids enhance the rate of hIAPP amyloid formation in mixed vesicles, but the effects are independent of the choice of zwitterionic lipids tested

We examined the effects of varying the percentage of anionic lipids, using mixed binary LUVs that contained differing amounts of anionic lipids, either DOPG or POPS, together with the zwitterionic lipid DOPC. We choose a lipid to peptide ratio of 20:1 and a hIAPP concentration of 20 μM for these and all following studies since this is typical of values used for biophysical studies of membrane catalyzed hIAPP amyloid formation [46, 52, 53]. This concentration will result in an excess of peptide relative to the concentration of vesicles. hIAPP has a T_{50}, defined as the time to reach 50 percent of the signal change in a thioflavin-T amyloid assay, of 42 hours in 20 mM tris in solution, in the absence of membranes under the conditions of our studies (Table-1).

Amyloid formation was followed using fluorescence thioflavin-T assays. Thioflavin-T is a small fluorescent dye whose quantum yield is low in solution, but is enhanced upon binding to amyloid fibrils. Thioflavin-T assays are a well-documented approach to follow hIAPP amyloid in solution and in the presence of membranes. Transmission electron microscopy (TEM) was used to visualize the final products of the amyloid formation assays to provide an independent test of amyloid formation. This is an important control since thioflavin-T is an extrinsic probe and sometimes gives a low signal even in the presence of amyloid fibrils [71]. As expected, and in agreement with earlier studies, the rate of hIAPP amyloid formation was notably enhanced in the presence of vesicles containing high percentages of anionic lipids (Figure-2) [42, 43, 49, 52, 57]. However, significant effects are observed for even modest amounts of DOPG or POPS. The addition of just 2 mole percent anionic lipid had a detectable effect, reducing the value of T_{50} by 10 percent for both POPS and DOPG relative to the value in the presence of vesicles that contained only zwitterionic lipids, and by 30 percent relative to value in the absence of vesicles. Addition of only 5 mole percent DOPG or POPS reduced T_{50} by almost 40 percent relative to the value in the presence of purely zwitterionic vesicles. Much larger effects were observed as the fraction of anionic lipids was increased with the value of T_{50} decreasing by over 90 percent with 50 mole percent anionic lipid (Figure-2, Table-1). Only modest differences were observed in the rate of amyloid formation when DOPG was substituted for POPS (Figure-2). The effect of POPS and DOPG are non-linear and are significant even at the lowest mole fractions tested (Figure-2). The data reveals that membranes with physiological concentrations of anionic lipids behave very differently than the systems commonly employed for biophysical studies, in which high concentrations of anionic lipids have been frequently used.

We next examined the effects of varying the zwitterionic lipid using POPS as the anionic lipid. Substitution of POPC for DOPC led to no significant differences in aggregation rates, as judged by the T_{50} values (Figure-S3). However, the choice of POPC vs DOPC did have an effect on the ability of hIAPP to induce leakage of vesicles, described below. TEM was used to probe the morphology of the amyloid fibrils which result from these experiments and the morphology of the vesicles. Vesicles containing only zwitterionic lipids and mixed

vesicles containing 25 mole percent anionic lipid and 75 mole percent zwitterionic lipid were examined. No detectable change in fibril morphology was observed at the level detectable by TEM and the presence of intact vesicles was confirmed (Figure-S4).

The addition of cholesterol reduces the ability of mixed anionic-zwitterionic LUVs to catalyze amyloid formation

Cholesterol is an important component of cellular membranes, and has been shown to be important for the uptake of IAPP by cells, however cholesterol is missing from, but not all, most commonly employed model vesicles used for IAPP studies of IAPP membrane interaction [51, 58]. The effects of varying the mole percent of cholesterol from 0 to 40 percent in the presence of POPC have been examined [51]. We examined the effects of cholesterol on membrane-catalyzed amyloid formation as a function of the percentage of cholesterol and POPS. LUVs composed of 0, 20 and 40 mole percent cholesterol with different amounts of POPS and POPC were studied. Cholesterol slowed the rate of fibril formation, consistent with prior results [51, 52] (Figure-3, Figure-S5). Recent studies conducted using a different buffer with an organic co-solvent (10 mM phosphate buffer, 100 mM NaCl, 1% DMSO), a different membrane composition and a different lipid to peptide ratio have also shown that cholesterol effects the rate of amyloid formation by IAPP. But in this case a modest acceleration was observed. Comparison of the data presented here with this study and with previous work [51, 52, 59] highlights the high sensitivity of IAPP membrane interactions to lipid composition. In the absence of POPS, addition of 20 mole percent cholesterol to zwitterionic LUVs increased the value of T_{50} by 1.5-fold relative to the value in the absence of cholesterol. Addition of 40 mole percent cholesterol further increased the value of T_{50} to 2.6-fold that of the no cholesterol value. Similarly, in the presence of moderate levels of POPS, 5 or 10 mole percent, the addition of 20 mole percent cholesterol increased T_{50} by more than 2-fold, while 40 mole percent cholesterol exhibited larger effects, increasing T_{50} by approximately 4-fold. However, added cholesterol had no detectable effect for the sample which contained 25 mole percent POPS, indicating that 25 mole percent POPS dominates cholesterol-dependent effects. This result indicates that studies which attempt to examine the effects of sterols on membrane mediated hIAPP amyloid formation should avoid moderate to high concentration of anionic lipids since they obscure the effects of cholesterol. TEM studies confirmed that the vesicles were intact at the end of the experiment and showed no significant change in fibril morphology (Figure-S4).

Sphingomyelin and POPC have similar effects on membrane catalyzed IAPP amyloid formation in the presence and absence of cholesterol

Sphingomyelin is an important component of biological membranes, and is found in the β-cell plasma membrane, but is usually not included in studies of hIAPP model membrane interactions. Thus, we examined the effects of sphingomyelin on membrane-catalyzed amyloid formation in the presence and absence of cholesterol with different amounts of POPC. Amyloid formation is slightly slower in samples which contain an equal molar mixture of brain sphingomyelin and POPC compared to pure POPC, both in the presence and absence of 40 mole percent cholesterol (Figure-S6, Table-1), but the effect is modest. Both egg and brain sphingomyelin are widely used in model membrane systems, consequently we compared the effects of varying the type of sphingomyelin using 50 percent

sphingomyelin and 50 percent POPC. A 16 to 20 percent increase in T_{50} was observed when brain sphingomyelin was replaced with egg sphingomyelin (Figure-S7, Table-1). TEM studies confirmed that the vesicles were intact at the end of the experiment and showed no significant change in fibril morphology (Figure-S4).

The choice of buffer or addition of NaCl significantly impacts membrane catalyzed amyloid formation, but the effects are different from those observed in ordinary aqueous solution

The rate of IAPP amyloid formation in solution depends upon the amount of salt present, and detectable effects are observed even at relatively modest ionic strengths. The rate is sensitive to the choice of anion, but less sensitive to the choice of the cation [72]. The salt dependence of hIAPP amyloid formation in solution depends upon Debye screening and anion binding at low to moderate salt concentrations with a contribution from Hofmeister effects at high salt concentrations [72]. Salts might have different effects in the membrane environment since adding salt can modulate peptide-membrane interactions as well as peptide-peptide interactions. Tris and phosphate are probably the most commonly employed buffers for biophysical studies of hIAPP amyloid formation, and phosphate accelerates amyloid formation in ordinary aqueous solution relative to tris. To the best of our knowledge, no systematic investigations have been reported on the effect of varying buffer composition on membrane catalyzed IAPP amyloid formation and very little is known about the effects of varying buffer on IAPP amyloid formation in homogenous solution. Thus, we explored the effects of adding 100 mM NaCl and changing the buffer from tris to phosphate on membrane catalyzed amyloid formation.

Addition of 100 mM NaCl to the tris buffer slowed amyloid formation in the presence of LUVs containing 25 mole percent POPS, increasing the value of T_{50} about 5-fold. This is the opposite of its effect in ordinary aqueous solution. Changing the buffer from 20 mM tris with no added salt to 20 mM phosphate with no added salt also slowed membrane catalyzed amyloid formation, increasing T_{50} by over 2-fold. Again, this is the opposite of the effects observed in solution. Adding 100 mM NaCl to phosphate buffer further slowed LUV catalyzed hIAPP amyloid formation, but the relative effect, less than 2-fold, was not as substantial as observed when NaCl was added to tris. Again, this is the opposite of its effect in aqueous solution. Varying the concentration of phosphate also had a significant effect: amyloid formation in the presence of LUVs containing 25 mole percent POPS was accelerated when the phosphate concentration was decreased from 20 mM to 10 mM (Figure-S8). In contrast, in aqueous solution decreasing the phosphate concentration decreases the rate of amyloid formation (data not shown). Collectively, the data reveal that changing buffer and the salt concentration have opposite effects on membrane catalyzed amyloid formation and on amyloid formation in homogenous solution. The opposing effects of added salt in solution vs in a membrane environment are consistent with electrostatic interactions playing an important role in the interaction of hIAPP with membranes containing anionic lipids, while the strong dependence on buffer composition indicates that caution is required when comparing studies conducted using different conditions.

hIAPP is more effective at permeabilizing LUVs which contain high concentrations of anionic lipids

We examined the effects of varying the amount of anionic lipid, DOPG or POPS, on membrane leakage using mixed binary LUVs with DOPC as the zwitterionic lipid. Membrane leakage was followed using fluorescence-detected 5(6)-carboxyfluorescein leakage assays. 5(6)-carboxyfluorescein is a highly fluorescent molecule whose fluorescence is self-quenched at high concentrations. High concentrations of the dye are encapsuled into LUVs, and upon membrane disruption by IAPP, the dye is released and the subsequent dilution leads to enhanced fluorescence. The percent membrane leakage is approximately equal to the percentage change in the fluorescence of the dye, although a plot of percent leakage vs percent change in dye fluorescence can deviate from linearity at higher dye concentrations (Figure-S2).

We measured leakage after 10 minutes of incubation and after incubating for a time long enough to form amyloid. Independent photochemical cross-linking and ion-mobility mass studies have shown that hIAPP forms oligomers in less than 10 minutes in solution of pH 7.4, while time resolved toxicity assays have shown that pre-amyloid oligomeric species are toxic to cultured INS-1 β-cells.[61, 73]

Inclusion of either POPS or DOPG in DOPC-containing vesicles increases the fluorescence change measured after 10 minutes relative to the change observed with pure DOPC vesicles, indicating increased leakage (Figure-4, Table-1, Figure-S9). This incubation time is noticeably less than the time required to from amyloid indicating that significant leakage is induced by, presumably, oligomeric species formed early in the amyloid self-assembly process. Incubating pure DOPC LUVs with hIAPP for 10 minutes led to a fluorescence increase of approximately 20 percent of maximal, while addition of just 2 mole percent of anionic lipid increased the fluorescence change to 36 percent of maximal, illustrating that even very modest fractions of anionic lipid led to detectable effects. Higher concentrations of anionic lipids lead to a larger change in 5(6)-carboxyfluorescein fluorescence. Addition of 50 mole percent of anionic lipid increased the observed fluorescence change to about 50–60 percent for both POPS and DOPG after 10 minutes of incubation with hIAPP. No clear differences were observed between dye release for vesicles containing POPS vs DOPG.

Dye leakage was also measured after 40 hours of incubation with hIAPP, which corresponds to a time after amyloid formation is finished for the samples which were slowest to form amyloid in the absence of cholesterol. The fluorescence increase was around 40 percent of maximal for the pure DOPC LUVs. Addition of 2 mole percent anionic lipid increased the change in 5(6)-carboxyfluorescein fluorescence to more than 50 percent, while addition of 50 mole percent of anionic lipid lead to release of almost all of the encapsulated dye. In summary, these studies demonstrate that increasing the mole fractions of anionic lipids leads to a significant increase in membrane leakage for both short and long incubation times with super physiological concentrations of anionic lipids leading to high levels of leakage.

Vesicles that contain POPC instead of DOPC are more resistant to hIAPP induced membrane leakage

We next examined the effects of varying the zwitterionic lipid on hIAPP induced membrane leakage using POPS as the anionic lipid. Although substitution of POPC for DOPC had only a modest impact on the rate of amyloid formation it did influence membrane leakage significantly. Greater leakage was observed for the DOPC vesicles relative to POPC containing LUVs for all concentrations of POPS tested at both the 10 minute and 40 hour incubation times (Figure-5, Table-1, Figure-S9). For vesicles lacking POPS or with a low POPS percentage, leakage at 10 minutes was 2 to 3 fold more for vesicles with DOPC relative to those with POPC. This difference decreased somewhat at higher POPS percentages (Figure-5A, Table-1). Similar, but somewhat smaller differences in leakage were observed after 40 hours of incubation time (Figure-5B, Table-1). The different effects observed with POPC vs DOPC likely reflects the differing abilities of these two lipids to pack owing to the double bond in both of the acyl chains of DOPC.

Cholesterol reduces the ability of hIAPP to induce membrane leakage

We examined the effects of cholesterol on hIAPP induced membrane leakage as a function of the percentage of cholesterol and POPS. LUVs made up of 0, 20 and 40 mole percent cholesterol with different amount of POPS and POPC were studied. Addition of cholesterol, at both 20 and 40 mole percent, reduced membrane leakage for all concentrations of POPS tested (Figure-6, Table-1, Figure-S10). The percentage change in 5(6)-carboxyfluorescein fluorescence increased as the mole percent of POPS increased for all conditions tested except for the 10 minute time point for the samples that contained 40 mole percent cholesterol. In that case no significant leakage was observed even for the sample which contained 25 mole percent POPS.

We also examined the samples after 120 hours of incubation. Amyloid formation is slowed in the presence of cholesterol, so we choose 120 hours instead of 40 hours to ensure that amyloid formation was complete. The relative reduction in leakage due to addition of 20 or 40 percent cholesterol was smaller for the 120 hour incubation times than for the 10 minute time point. Six percent leakage was observed for the vesicles with 40 mole percent cholesterol and no POPS, while 38 percent leakage was observed from vesicles that contained 40 mole percent cholesterol and 25 mole percent POPS (Figure-6B, Table-1). For comparison, the corresponding values for 0 mole percent cholesterol were 25 and 56 percent respectively.

Replacement of POPC with brain sphingomyelin decreases vesicle leakage in the absence and in the presence of cholesterol

We next examined the effects of replacing POPC with sphingomyelin on hIAPP induced membrane leakage for LUVs in the presence and absence of cholesterol. More leakage was detected for the pure POPC LUVs compared to LUVs that were made up of a 50 mole percent mixture of POPC and brain sphingomyelin after both 10 minutes and 120 hours incubation time. No significant difference in dye leakage was observed upon substituting brain sphingomyelin for egg sphingomyelin (Figure-S11, Table-1).

Different results were obtained when 10 mole percent POPS was present. No detectable difference in the apparent leakage was observed when comparing LUVs composed of 90 mole percent POPC and 10 mole percent POPS to LUVs containing 60 mole percent POPC, 30 mole percent brain sphingomyelin, and 10 mole percent POPS (Table-1). This result further highlights the significant effect of even modest amounts of anionic lipids. The estimated mole percentage of POPS in the β-cell membrane is below 10 percent, thus even just 10 percent POPS represents a poor mimic of the outer leaflet of the β-cell plasma membrane. The addition of sphingomyelin also had an effect upon vesicles composed of POPC and cholesterol, reducing the leakage observed after 120 hours incubation (Figure-S11, Table-1).

A correlation between leakage and peptide binding to vesicles

The observed percentage leakage does not reach 100%, and for some lipid compositions leakage remains at a low level for very long times even though hIAPP is added in excess in these experiments. A possible explanation is that a subset of the LUVs binds peptide and a fraction does not, or binds fewer peptides under the conditions of these studies. We conducted sucrose gradient experiments to test this possibility using LUVs that experience a high degree of membrane permeability and LUVs that do not. LUVs labeled at 2 mole percent with the fluorescence probe NBD-DOPE were centrifuged in a 5 to 20 percent sucrose gradient. Two fractions were observed in the presence of IAPP, a lighter fraction which floats at the top of the gradient in the same position observed for control LUVs in the absence of peptide, and a second fraction which pellets. Because vesicle-bound peptides increase vesicle density, the lighter fraction contains vesicles with little IAPP while those with a high peptide content form the heavier fraction that pellets. The sucrose gradient experiments reveal that not all vesicles bind peptide even though hIAPP is present in excess. This may be due to cooperative binding of hIAPP, so that it preferentially binds to a subset of vesicles. In addition, once amyloid fibrils are formed they might compete with membranes for the remaining soluble hIAPP and thereby limit the interactions of the soluble pool of hIAPP with LUVs. There is a strong correlation between the fraction of vesicles pelleted, i.e. those which bound peptide, and the observed leakage (Figure-S12, Table-1). This confirms that the extent of leakage reflects the fraction of vesicles that bind substantial amounts of peptide.

h-Amylin induces leakage via pore formation

The experiments described above have examined the effect of varying lipid composition on vesicle leakage, but they do not address the mechanism of leakage. The release of the 5(6)-carboxyfluorescein dye could be due to formation of pores and / or more complete disruption of the vesicles by a detergent like mechanism. We conducted FRET experiments with labeled lipids to probe the intactness of the vesicles after incubation with hIAPP (Figure-S13). A small percentage of donor lipid (0.5 mole percent NBD-DOPE) and acceptor lipid (1 mole percent Rho-DOPE) were incorporated into the vesicles. Efficient FRET is observed in intact vesicles since the donor and the acceptor are in proximity. The FRET signal will be diminished if the vesicles are fully disrupted so that the lipids are solubilized and no longer in close proximity. In the absence of hIAPP significant FRET was observed with F/Fo = 0.2 (corresponding to 80% FRET efficiency) for pure POPC samples

without cholesterol. Fo is the fluorescence of vesicles which contain the donor lipid, but not the acceptor lipid and F is the fluorescence of vesicles which have both donor and acceptor lipids. The observed value is consistent with the Förster radius and the estimated donor acceptor separation[74]. The F/Fo value is 0.4 (corresponding to 60% FRET efficiency) for POPC samples with 20 mole percent cholesterol. As a control, we used triton X-100 to disrupt the vesicles and found that F/Fo was 0.9 (10% FRET efficiency), indicating, as expected, that FRET was significantly reduced when the vesicles were disrupted. We then examined the effect of treating POPC vesicles with h-amylin and found no change in FRET efficiency with or without 20 mole percent both after both10 minutes or 2 days of incubation (Figure-S13). Similar results were observed with vesicles composed of 3:1 POPC : POPS. We choose this vesicle composition because it provides an example of a system which shows very significant levels of leakage. This set of experiments argues that 5(6)-carboxyfluorescein release does not involve complete solubilization of the vesicles. DLS was used to probe the integrity of the vesicles after 10 minutes incubation with hIAPP and confirmed the presence of intact vesicles (Table-S1).

The FRET studies are consistent with formation of some sort of pore, but they do not provide information about pore size. Consequently, we studied the ability of hIAPP to induce leakage of different sized fluorescence probes. We used a set of dextrans conjugated to fluorescein isothiocyanate (FITC-dextran) of different sizes ranging from 5 kDa to 150 kDa. Three sets of vesicles were prepared; pure POPC vesicles, vesicles composed of 75 mole percent POPC with 25 mole percent POPS and vesicles made up of 80 mole percent POPC with 20 mole percent of cholesterol. Dextran leakage was measured after 10 min, 1 h and 80 h of incubation with hIAPP. Significant leakage was observed for all samples, with slightly less leakage detected for higher molecular weight FITC-dextran. Dextran leakage was also slightly less than the leakage of 5(6)-carboxyfluorescein (which is smaller than all of the dextrans used) at the same incubation time (Figure-7). This indicates that average pore size is large, although it may be somewhat variable from vesicle-to-vesicle. The studies indicate that pore formation plays an important role in leakage, but do not distinguish between transiently formed pores or persistent pores.

DISCUSSION

The data presented here highlights the sensitivity of membrane-catalyzed hIAPP amyloid formation and the ability of hIAPP to permeabilize membranes to membrane composition. The strong non-linear dependence on the fraction of anionic lipid, and on the presence or absence of cholesterol demonstrated in our study has clear implications for the design of model membranes for biophysical studies. The data presented here shows that significant effects are observed even at the lowest level of anionic lipids. Addition of just 2 mole percent anionic lipid lead to a measurable effect. Anionic lipids are estimated to make up between 2.5 to 13.2 percent of the total phospholipid in the β-cell plasma membrane and are localized to the inner leaflet, however, the actual concentration of anionic lipids is lower since the membrane contains significant amounts of cholesterol. Overall, anionic lipids likely make up between 1.5 to 8 mole percent of the membrane. Figure-2C reveals that increasing the concentration of anionic lipids from 8 mole percent to just 25 mole percent, the latter being a value used in model membrane studies, has a dramatic effect, reducing the

T_{50} for the POPS containing binary LUVs by a factor of 5. 25 mole percent POPS is on the low side of the values used in many biophysical studies.

The detailed molecular mechanism of membrane enhanced amyloid formation is not understood, but it is likely related to specific structures formed on the membrane coupled with a reduction in dimensionality. hIAPP is thought to bind to membranes in a partial helical conformation and then associate on the membranes to form helical oligomeric structures which convert into β-sheet rich amyloid fibrils by an unknown mechanism [56, 75–81]. Binding increases the local concentration of hIAPP and reduces hIAPP-hIAPP interactions to a two dimensional search. Faster aggregation is expected as the fraction of anionic lipids increases due to enhanced binding of the cationic peptide, but at sufficiently high concentrations of anionic lipids and at appropriate peptide to lipid ratios conversion to β-sheet structure could be slowed if interactions with a highly charged membrane over-stabilized the helical state[56]. Irrespective of the mechanism details, the present study clearly demonstrates that model membranes containing significant anionic lipids act very differently than membranes which contain physiologically relevant levels of anionic lipids.

A number of structures of hIAPP in membrane-mimetic environments have been reported based on NMR and EPR studies which are consistent with a role for α-helix formation during membrane catalyzed hIAPP amyloid formation. The structures differ in some of the details, but they all report a well ordered α-helix beginning near residue 7 and continuing to somewhere between residues 18 to 22 [76–78, 80]. Formation of an amphipathic helix in this region positions Arg-11 and His-18 on the same face of the helix [76, 78]. The Cys-2 Cys-7 disulfide bond prevents the N-terminal region from adopting a canonical α-helix structure, however NMR studies of hIAPP in micelles indicate that the N-terminal region can from a structure which places Lys-1 on the same face of the structure as Arg-11 and His-18 [77, 80]. This constellation of cationic residues will promote electrostatic interactions of hIAPP with anionic vesicles, and micelles and helps to rationalize the sensitivity of membrane-catalyzed amyloid formation to the fraction of anionic lipids. The salt dependent studies and the opposing effects of added salt on IAPP amyloid formation in solution vs in the membrane environment are consistent with electrostatic interactions playing an important role in membrane hIAPP interactions.

Cholesterol also had a significant effect, but in this case slowed amyloid formation. The contrasting effects of cholesterol and anionic lipids on membrane catalyzed amyloid formation and on hIAPP induced membrane leakage are noteworthy. An important observation in the present work is that the relative effect of adding cholesterol on amyloid formation is much less in the presence of 25 mole percent POPS. This highlights the strong influence anionic lipids have on IAPP amyloid formation and indicates that caution must be employed when studying the effect of other components in the presence of high concentrations of anionic lipids, since they can dominate the more subtle effects induced by varying other components. Further evidence of the complicating effects of high concentrations of anionic lipids are provided by the studies of the effect of sphingomyelin on vesicle leakage. Sphingomyelin decreased leakage in the absence of POPS, but adding sphingomyelin had no effect when 10 mole percent POPS was present. These experiments

reinforce the important fact that hIAPP experiences very different environments when interacting with the outer leaflet of the β-cell plasma membrane, with its reduced anionic lipid content, vs the inner leaflet with its higher anionic lipid content.

Membrane-catalyzed amyloid formation was largely independent of the choice of zwitterionic lipids including POPC, DOPC and sphingomyelin for the conditions studied here. This implies that the rate of amyloid formation is not strongly dependent on lipid acyl chain saturation, and is most easily rationalized by models which invoke hIAPP binding in an orientation perpendicular to the bilayer normal, since IAPP will interact with the headgroups in this orientation and does not have to significantly penetrate the membrane to form amyloid. In contrast, the extent of leakage was dependent on the choice of zwitterionic lipid with more leakage observed for lipids that form less ordered bilayers. The increased sensitivity of leakage to membrane composition likely reflects the requirement that hIAPP needs to insert into the membrane to promote leakage.

The salt and buffer dependent studies reveal that hIAPP membrane mediated amyloid formation is very sensitive to conditions and show that adding NaCl or changing buffer has different effects on amyloid formation in the presence of LUVs compared to their effects in homogenous solution. The differences reflect a competition between the effects of anions and salt on hIAPP-hIAPP interactions vs hIAPP-membrane interactions. Salts screen unfavorable hIAPP-hIAPP electrostatic interactions thereby speeding up aggregation in solution, but can reduce IAPP-membrane electrostatic interactions that promote amyloid formation, at least for vesicles containing anionic lipids. The net effect, under the conditions used here, is to slow membrane catalyzed amyloid formation by anionic LUVs. An important practical point is that minor variations in buffer or salt composition or concentration have a significant effect on hIAPP membrane interactions, making comparison of studies conducted under different conditions challenging. Low levels of $Ca^{2+,}$ also have significant effects upon hIAPP amyloid formation in the presence of anionic vesicles, but in this case the mechanism is different and the effects are due to cation binding to the head group of the anionic lipids [82].

The observation that even low levels of POPS promote amyloid formation and facilitate hIAPP induced leakage has potentially interesting biologically implications. It is known that that toxic hIAPP oligomers produced during amyloid formation induce apoptosis [11, 20], and that apoptosis leads to a break down in membrane asymmetry of phosphatidylserine (PS) [83–85]. The loss of asymmetry could be due to a direct effect of hIAPP if it leads to membrane permeabilization, and permeabilization reduces PS asymmetry. Alternatively, the loss of PS asymmetry could be an indirect consequence of apoptosis induced by some other aspect of hIAPP toxicity. In either case this could lead to a feedback loop in which increased PS in the outer leaflet in one cell could promote additional formation of toxic hIAPP species, and additional deleterious hIAPP-membrane interactions, not necessarily involving the same cell. This would in turn result in further transfer of PS to the outer leaflet. Since the presence of PS in the outer leaflet promotes macrophage mediated destruction of cells, a breakdown in membrane asymmetry could also contribute to macrophage mediated loss of β-cells [86–88]. Differentiating between these possibilities is beyond the scope of the present work.

The ability of hIAPP to induce leakage appears to be even more sensitive to membrane composition than amyloid formation since varying some membrane components had a clearly measurable effect on membrane permeability, but not on the kinetics of amyloid formation. Collectively the data indicates that factors which lead to more ordered membranes [89], such as cholesterol or sphingomyelin or the replacement of DOPC with POPC reduce the susceptibility of model membranes to hIAPP induced leakage although this effect can be overcome when anionic lipid is present.

The observation of significant vesicle leakage after only 10 minutes of incubation for the systems studied here is consistent with the hypothesis that species populated during the lag phase are membrane-active since 10 minutes is significantly less than the time required to form amyloid in the presence of LUVs except for the samples with 50 percent anionic lipid. Nevertheless, a correlation is observed between T_{50} and the leakage detected after 10 minutes of incubation. (Figure-8). The correlation likely arises because more effective hIAPP-membrane interactions promote more rapid amyloid formation and effective membrane interactions are also required to promote leakage. A stronger correlation is observed between the values of T_{50} and the extent of leakage measured after incubating for a time long enough to ensure that amyloid formation is complete (Figure-8). The correlation is even more striking if just the POPS plus POPC data is plotted, or if the data for the cholesterol dependent studies are examined separately (Figure-S14). The FRET studies and dextran leakage experiments demonstrate the dominate mechanism of leakage under the conditions used here is pore formation and reveals that the pores are of large diameter.

Supplementary Material

Refer to Web version on PubMed Central for supplementary material.

Acknowledgments

We thank members of the London and Raleigh labs for helpful discussions.

Funding

This work was supported by NIH grants GM078114 (D.P.R) and GM112638 (E.L.).

ABBREVIATIONS

DLS	dynamic light scattering
DMSO	dimethyl sulfoxide
DOPC	1,2-dioleoyl-sn-glycero-3-phosphocholine
DOPG	1,2-dioleoyl-sn-glycero-3-phospho-(1'-rac-glycerol)
DOPS	1,2-dioleoyl-sn-glycero-3-phospho-L-serine
FITC-dextran	fluorescein isothiocyanate–dextran
Fmoc	fluoronylmethoxycarbonyl

FRET	Förster resonance energy transfer
HFIP	hexafluoroisopropanol
hIAPP	human islet amyloid polypeptide
HPLC	high performance liquid chromatography
IAPP	islet amyloid polypeptide
LUV	large unilamellar vesicles
MALDI-TOF	time-of-flight matrix-assisted laser desorption ionization
MLV	multilamellar vesicles
NBD-DOPE	1,2-dioleoyl-sn-glycero-3-phosphoethanolamine-N-(7-nitro-2-1,3-benzoxadiazol-4-yl)
POPC	1-palmitoyl-2-oleoyl-sn-glycero-3-phosphocholine
POPS	1-palmitoyl-2-oleoyl-sn-glycero-3-phospho-L-serine
PS	phosphatidylserine
Rho-DOPE	1,2-dioleoyl-sn-glycero-3-phosphoethanolamine-N-(lissamine rhodamine B sulfonyl)
T2D	type-2 diabetes
T_{50}	the time to reach 50% of the signal change in a thioflavin-T amyloid assay
TEM	transmission electron microscopy
TFA	trifluoroacetic acid

References

1. Hay DL, Chen S, Lutz TA, Parkes DG, Roth JD. Amylin: pharmacology, physiology, and clinical potential. Pharmacol Rev. 2015; 67:564–600. [PubMed: 26071095]
2. Westermark P, Wernstedt C, Wilander E, Hayden DW, O'Brien TD, Johnson KH. Amyloid fibrils in human insulinoma and islets of Langerhans of the diabetic cat are derived from a neuropeptide-like protein also present in normal islet cells. Proc Natl Acad Sci U S A. 1987; 84:3881–3885. [PubMed: 3035556]
3. Cooper GJ, Willis AC, Clark A, Turner RC, Sim RB, Reid KB. Purification and characterization of a peptide from amyloid-rich pancreases of type 2 diabetic patients. Proc Natl Acad Sci U S A. 1987; 84:8628–8632. [PubMed: 3317417]
4. Clark A, Cooper GJ, Lewis CE, Morris JF, Willis AC, Reid KB, Turner RC. Islet amyloid formed from diabetes-associated peptide may be pathogenic in type-2 diabetes. Lancet (London, England). 1987; 2:231–234.
5. Hull RL, Westermark GT, Westermark P, Kahn SE. Islet amyloid: a critical entity in the pathogenesis of type 2 diabetes. J Clin Endocrinol Metab. 2004; 89:3629–3643. [PubMed: 15292279]

6. Lorenzo A, Razzaboni B, Weir GC, Yankner BA. Pancreatic islet cell toxicity of amylin associated with type-2 diabetes mellitus. Nature. 1994; 368:756–760. [PubMed: 8152488]
7. Kahn SE, Andrikopoulos S, Verchere CB. Islet amyloid: a long-recognized but underappreciated pathological feature of type 2 diabetes. Diabetes. 1999; 48:241–253. [PubMed: 10334297]
8. Clark A, Wells CA, Buley ID, Cruickshank JK, Vanhegan RI, Matthews DR, Cooper GJ, Holman RR, Turner RC. Islet amyloid, increased A-cells, reduced B-cells and exocrine fibrosis: quantitative changes in the pancreas in type 2 diabetes. Diabetes Res. 1988; 9:151–159. [PubMed: 3073901]
9. de Koning EJ, Bodkin NL, Hansen BC, Clark A. Diabetes mellitus in Macaca mulatta monkeys is characterised by islet amyloidosis and reduction in beta-cell population. Diabetologia. 1993; 36:378–384. [PubMed: 8314440]
10. Loomes KM. Survival of an islet beta-cell in type-2 diabetes: curbing the effects of amyloid cytotoxicity. Islets. 2011; 3:38–39. [PubMed: 21266844]
11. Westermark P, Andersson A, Westermark GT. Islet amyloid polypeptide, islet amyloid, and diabetes mellitus. Physiol Rev. 2011; 91:795–826. [PubMed: 21742788]
12. Jurgens CA, Toukatly MN, Fligner CL, Udayasankar J, Subramanian SL, Zraika S, Aston-Mourney K, Carr DB, Westermark P, Westermark GT, Kahn SE, Hull RL. beta-cell loss and beta-cell apoptosis in human type 2 diabetes are related to islet amyloid deposition. Am J Pathol. 2011; 178:2632–2640. [PubMed: 21641386]
13. Kahn SE, Zraika S, Utzschneider KM, Hull RL. The beta cell lesion in type 2 diabetes: there has to be a primary functional abnormality. Diabetologia. 2009; 52:1003–1012. [PubMed: 19326096]
14. Zraika S, Hull RL, Verchere CB, Clark A, Potter KJ, Fraser PE, Raleigh DP, Kahn SE. Toxic oligomers and islet beta cell death: guilty by association or convicted by circumstantial evidence? Diabetologia. 2010; 53:1046–1056. [PubMed: 20182863]
15. Cooper GJ, Aitken JF, Zhang S. Is type 2 diabetes an amyloidosis and does it really matter (to patients)? Diabetologia. 2010; 53:1011–1016. [PubMed: 20229094]
16. Masters SL, Dunne A, Subramanian SL, Hull RL, Tannahill GM, Sharp FA, Becker C, Franchi L, Yoshihara E, Chen Z, Mullooly N, Mielke LA, Harris J, Coll RC, Mills KH, Mok KH, Newsholme P, Nunez G, Yodoi J, Kahn SE, Lavelle EC, O'Neill LA. Activation of the NLRP3 inflammasome by islet amyloid polypeptide provides a mechanism for enhanced IL-1beta in type 2 diabetes. Nat Immunol. 2010; 11:897–904. [PubMed: 20835230]
17. Akter R, Cao P, Noor H, Ridgway Z, Tu L-H, Wang H, Wong AG, Zhang X, Abedini A, Schmidt AM, Raleigh DP. Islet amyloid polypeptide: structure, function, and pathophysiology. J Diabetes Res. 2016; 2016:18.
18. Cao P, Abedini A, Raleigh DP. Aggregation of islet amyloid polypeptide: from physical chemistry to cell biology. Curr Opin Struct Biol. 2013; 23:82–89. [PubMed: 23266002]
19. Cao P, Marek P, Noor H, Patsalo V, Tu LH, Wang H, Abedini A, Raleigh DP. Islet amyloid: from fundamental biophysics to mechanisms of cytotoxicity. FEBS Lett. 2013; 587:1106–1118. [PubMed: 23380070]
20. Abedini A, Schmidt AM. Mechanisms of islet amyloidosis toxicity in type 2 diabetes. FEBS Lett. 2013; 587:1119–1127. [PubMed: 23337872]
21. Montane J, Klimek-Abercrombie A, Potter KJ, Westwell-Roper C, Bruce Verchere C. Metabolic stress, IAPP and islet amyloid. Diabetes Obes Metab. 2012; 14(Suppl 3):68–77. [PubMed: 22928566]
22. Phillips LK, Horowitz M. Amylin. Curr Opin Endocrinol Diabetes Obes. 2006; 13:191–198.
23. Lutz TA. The role of amylin in the control of energy homeostasis. Am J Physiol Regul Integr Comp Physiol. 2010; 298:R1475–1484. [PubMed: 20357016]
24. Rushing PA, Hagan MM, Seeley RJ, Lutz TA, D'Alessio DA, Air EL, Woods SC. Inhibition of central amylin signaling increases food intake and body adiposity in rats. Endocrinology. 2001; 142:5035. [PubMed: 11606473]
25. Ashcroft FM, Rorsman P. Diabetes mellitus and the beta cell: the last ten years. Cell. 2012; 148:1160–1171. [PubMed: 22424227]
26. Halban PA, Polonsky KS, Bowden DW, Hawkins MA, Ling C, Mather KJ, Powers AC, Rhodes CJ, Sussel L, Weir GC. beta-cell failure in type 2 diabetes: postulated mechanisms and prospects for prevention and treatment. Diabetes Care. 2014; 37:1751–1758. [PubMed: 24812433]

27. Matveyenko AV, Butler PC. Beta-cell deficit due to increased apoptosis in the human islet amyloid polypeptide transgenic (HIP) rat recapitulates the metabolic defects present in type 2 diabetes. Diabetes. 2006; 55:2106–2114. [PubMed: 16804082]
28. Westermark GT, Westermark P, Berne C, Korsgren O, Nordic Network for Clinical Islet T. Widespread amyloid deposition in transplanted human pancreatic islets. N Engl J Med. 2008; 359:977–979. [PubMed: 18753660]
29. Udayasankar J, Kodama K, Hull RL, Zraika S, Aston-Mourney K, Subramanian SL, Tong J, Faulenbach MV, Vidal J, Kahn SE. Amyloid formation results in recurrence of hyperglycaemia following transplantation of human IAPP transgenic mouse islets. Diabetologia. 2009; 52:145–153. [PubMed: 19002432]
30. Potter KJ, Abedini A, Marek P, Klimek AM, Butterworth S, Driscoll M, Baker R, Nilsson MR, Warnock GL, Oberholzer J, Bertera S, Trucco M, Korbutt GS, Fraser PE, Raleigh DP, Verchere CB. Islet amyloid deposition limits the viability of human islet grafts but not porcine islet grafts. Proc Natl Acad Sci U S A. 2010; 107:4305–4310. [PubMed: 20160085]
31. Despa S, Margulies KB, Chen L, Knowlton AA, Havel PJ, Taegtmeyer H, Bers DM, Despa F. Hyperamylinemia contributes to cardiac dysfunction in obesity and diabetes: a study in humans and rats. Circ Res. 2012; 110:598–608. [PubMed: 22275486]
32. Despa S, Sharma S, Harris TR, Dong H, Li N, Chiamvimonvat N, Taegtmeyer H, Margulies KB, Hammock BD, Despa F. Cardioprotection by controlling hyperamylinemia in a “humanized” diabetic rat model. J Am Heart Assoc. 2014; 3
33. Janson J, Ashley RH, Harrison D, McIntyre S, Butler PC. The mechanism of islet amyloid polypeptide toxicity is membrane disruption by intermediate-sized toxic amyloid particles. Diabetes. 1999; 48:491–498. [PubMed: 10078548]
34. Zhang S, Liu J, Dragunow M, Cooper GJ. Fibrillogenic amylin evokes islet beta-cell apoptosis through linked activation of a caspase cascade and JNK1. J Biol Chem. 2003; 278:52810–52819. [PubMed: 14532296]
35. Subramanian SL, Hull RL, Zraika S, Aston-Mourney K, Udayasankar J, Kahn SE. cJUN N-terminal kinase (JNK) activation mediates islet amyloid-induced beta cell apoptosis in cultured human islet amyloid polypeptide transgenic mouse islets. Diabetologia. 2012; 55:166–174. [PubMed: 22038516]
36. Park YJ, Lee S, Kieffer TJ, Warnock GL, Safikhan N, Speck M, Hao Z, Woo M, Marzban L. Deletion of Fas protects islet beta cells from cytotoxic effects of human islet amyloid polypeptide. Diabetologia. 2012; 55:1035–1047.
37. Rivera JF, Gurlo T, Daval M, Huang CJ, Matveyenko AV, Butler PC, Costes S. Human-IAPP disrupts the autophagy/lysosomal pathway in pancreatic beta-cells: protective role of p62-positive cytoplasmic inclusions. Cell Death Differ. 2011; 18:415–426. [PubMed: 20814419]
38. Zraika S, Hull RL, Udayasankar J, Aston-Mourney K, Subramanian SL, Kisilevsky R, Szarek WA, Kahn SE. Oxidative stress is induced by islet amyloid formation and time-dependently mediates amyloid-induced beta cell apoptosis. Diabetologia. 2009; 52:626–635. [PubMed: 19148619]
39. Mirzabekov TA, Lin MC, Kagan BL. Pore formation by the cytotoxic islet amyloid peptide amylin. J Biol Chem. 1996; 271:1988–1992. [PubMed: 8567648]
40. Anguiano M, Nowak RJ, Lansbury PT. Protofibrillar islet amyloid polypeptide permeabilizes synthetic vesicles by a pore-like mechanism that may be relevant to type II diabetes. Biochemistry. 2002; 41:11338–11343. [PubMed: 12234175]
41. Sparr E, Engel MF, Sakharov DV, Sprong M, Jacobs J, de Kruijff B, Hoppener JW, Killian JA. Islet amyloid polypeptide-induced membrane leakage involves uptake of lipids by forming amyloid fibers. FEBS Lett. 2004; 577:117–120. [PubMed: 15527771]
42. Brender JR, Salamekh S, Ramamoorthy A. Membrane disruption and early events in the aggregation of the diabetes related peptide IAPP from a molecular perspective. Acc Chem Res. 2012; 45:454–462. [PubMed: 21942864]
43. Hebda JA, Miranker AD. The interplay of catalysis and toxicity by amyloid intermediates on lipid bilayers: insights from type II diabetes. Annu Rev Biophys. 2009; 38:125–152. [PubMed: 19416063]

44. Engel MF. Membrane permeabilization by islet amyloid polypeptide. Chem Phys Lipids. 2009; 160:1–10. [PubMed: 19501206]
45. Porat Y, Kolusheva S, Jelinek R, Gazit E. The human islet amyloid polypeptide forms transient membrane-active prefibrillar assemblies. Biochemistry. 2003; 42:10971–10977. [PubMed: 12974632]
46. Last NB, Rhoades E, Miranker AD. Islet amyloid polypeptide demonstrates a persistent capacity to disrupt membrane integrity. Proc Natl Acad Sci U S A. 2011; 108:9460–9465. [PubMed: 21606325]
47. Engel MF, Khemtemourian L, Kleijer CC, Meeldijk HJ, Jacobs J, Verkleij AJ, de Kruijff B, Killian JA, Hoppener JW. Membrane damage by human islet amyloid polypeptide through fibril growth at the membrane. Proc Natl Acad Sci U S A. 2008; 105:6033–6038. [PubMed: 18408164]
48. Sciacca MF, Brender JR, Lee DK, Ramamoorthy A. Phosphatidylethanolamine enhances amyloid fiber-dependent membrane fragmentation. Biochemistry. 2012; 51:7676–7684. [PubMed: 22970795]
49. Jayasinghe SA, Langen R. Lipid membranes modulate the structure of islet amyloid polypeptide. Biochemistry. 2005; 44:12113–12119. [PubMed: 16142909]
50. Wang H, Cao P, Raleigh DP. Amyloid formation in heterogeneous environments: islet amyloid polypeptide glycosaminoglycan interactions. J Mol Biol. 2013; 425:492–505. [PubMed: 23154166]
51. Caillon L, Duma L, Lequin O, Khemtemourian L. Cholesterol modulates the interaction of the islet amyloid polypeptide with membranes. Mol Membr Biol. 2014; 31:239–249. [PubMed: 25495656]
52. Caillon L, Lequin O, Khemtemourian L. Evaluation of membrane models and their composition for islet amyloid polypeptide-membrane aggregation. Biochim Biophys Acta. 2013; 1828:2091–2098. [PubMed: 23707907]
53. Kegulian NC, Sankhagowit S, Apostolidou M, Jayasinghe SA, Malmstadt N, Butler PC, Langen R. Membrane curvature-sensing and curvature-inducing activity of islet amyloid polypeptide and its implications for membrane disruption. J Biol Chem. 2015; 290:25782–25793. [PubMed: 26283787]
54. Cao P, Abedini A, Wang H, Tu LH, Zhang X, Schmidt AM, Raleigh DP. Islet amyloid polypeptide toxicity and membrane interactions. Proc Natl Acad Sci U S A. 2013; 110:19279–19284. [PubMed: 24218607]
55. Abedini A, Tracz SM, Cho JH, Raleigh DP. Characterization of the heparin binding site in the N-terminus of human pro-islet amyloid polypeptide: implications for amyloid formation. Biochemistry. 2006; 45:9228–9237. [PubMed: 16866369]
56. Apostolidou M, Jayasinghe SA, Langen R. Structure of alpha-helical membrane-bound human islet amyloid polypeptide and its implications for membrane-mediated misfolding. J Biol Chem. 2008; 283:17205–17210. [PubMed: 18442979]
57. Seeliger J, Weise K, Opitz N, Winter R. The effect of Abeta on IAPP aggregation in the presence of an isolated beta-cell membrane. J Mol Biol. 2012; 421:348–363. [PubMed: 22321797]
58. Trikha S, Jeremic AM. Clustering and internalization of toxic amylin oligomers in pancreatic cells require plasma membrane cholesterol. J Biol Chem. 2011; 286:36086–36097. [PubMed: 21865171]
59. Sciacca, Michele FM., Lolicato, F., Di Mauro, G., Milardi, D., D'Urso, L., Satriano, C., Ramamoorthy, A., La Rosa, C. The role of cholesterol in driving IAPP-membrane interactions. Biophysical Journal. 2016; 111:140–151. [PubMed: 27410742]
60. London E. Insights into lipid raft structure and formation from experiments in model membranes. Curr Opin Struct Biol. 2002; 12:480–486. [PubMed: 12163071]
61. Abedini A, Plesner A, Cao P, Ridgway Z, Zhang J, Tu LH, Middleton CT, Chao B, Sartori DJ, Meng F, Wang H, Wong AG, Zanni MT, Verchere CB, Raleigh DP, Schmidt AM. Time-resolved studies define the nature of toxic IAPP intermediates, providing insight for anti-amyloidosis therapeutics. Elife. 2016; 5:e12977. [PubMed: 27213520]
62. Aston-Mourney K, Hull RL, Zraika S, Udayasankar J, Subramanian SL, Kahn SE. Exendin-4 increases islet amyloid deposition but offsets the resultant beta cell toxicity in human islet amyloid polypeptide transgenic mouse islets. Diabetologia. 2011; 54:1756–1765. [PubMed: 21484213]

63. Abedini A, Raleigh DP. Incorporation of pseudoproline derivatives allows the facile synthesis of human IAPP, a highly amyloidogenic and aggregation-prone polypeptide. Org Lett. 2005; 7:693–696. [PubMed: 15704927]
64. Marek P, Woys AM, Sutton K, Zanni MT, Raleigh DP. Efficient microwave-assisted synthesis of human islet amyloid polypeptide designed to facilitate the specific incorporation of labeled amino acids. Org Lett. 2010; 12:4848–4851. [PubMed: 20931985]
65. Abedini A, Singh G, Raleigh DP. Recovery and purification of highly aggregation-prone disulfide-containing peptides: application to islet amyloid polypeptide. Anal Biochem. 2006; 351:181–186. [PubMed: 16406209]
66. Nilsson MR, Raleigh DP. Analysis of amylin cleavage products provides new insights into the amyloidogenic region of human amylin. J Mol Biol. 1999; 294:1375–1385. [PubMed: 10600392]
67. Nilsson MR, Driscoll M, Raleigh DP. Low levels of asparagines deamidation can have a dramatic effect on aggregation of amyloidogenic peptides: implications for the study of amyloid formation. Protein Sci. 2002; 11:342–349. [PubMed: 11790844]
68. Dunkelberger EB, Buchanan LE, Marek P, Cao P, Raleigh DP, Zanni MT. Deamidation accelerates amyloid formation and alters amylin fiber structure. J Am Chem Soc. 2012; 134:12658–12667. [PubMed: 22734583]
69. Stewart JC. Colorimetric determination of phospholipids with ammonium ferrothiocyanate. Anal Biochem. 1980; 104:10–14. [PubMed: 6892980]
70. Lin Q, Wang T, Li H, London E. Decreasing transmembrane segment length greatly decreases perfringolysin O pore size. J Membrane Biol. 2015; 248:517–527. [PubMed: 25850715]
71. Wong AG, Wu C, Hannaberry E, Watson MD, Shea JE, Raleigh DP. Analysis of the amyloidogenic potential of pufferfish (Takifugu rubripes) islet amyloid polypeptide highlights the limitations of thioflavin-T assays and the difficulties in defining amyloidogenicity. Biochemistry. 2016; 55:510–518. [PubMed: 26694855]
72. Marek PJ, Patsalo V, Green DF, Raleigh DP. Ionic strength effects on amyloid formation by amylin are a complicated interplay among Debye screening, ion selectivity, and Hofmeister effects. Biochemistry. 2012; 51:8478–8490. [PubMed: 23016872]
73. Young LM, Cao P, Raleigh DP, Ashcroft AE, Radford SE. Ion mobility spectrometry-mass spectrometry defines the oligomeric intermediates in amylin amyloid formation and the mode of action of inhibitors. J Am Chem Soc. 2014; 136:660–670. [PubMed: 24372466]
74. Pathak P, London E. Measurement of lipid nanodomain (raft) formation and size in sphingomyelin/POPC/cholesterol vesicles shows TX-100 and transmembrane helices increase domain size by coalescing preexisting nanodomains but do not induce domain formation. Biophys J. 2011; 101:2417–2425. [PubMed: 22098740]
75. Nanga RPR. Structures of rat and human islet amyloid polypeptide IAPP(1–19) in micelles by NMR spectroscopy. Biochemistry. 2008; 47:12689–12697. [PubMed: 18989932]
76. Breeze AL, Harvey TS, Bazzo R, Campbell ID. Solution structure of human calcitonin gene-related peptide by 1H NMR and distance geometry with restrained molecular dynamics. Biochemistry. 1991; 30:575–582. [PubMed: 1988044]
77. Nanga RPR, Brender JR, Vivekanandan S, Ramamoorthy A. Structure and membrane orientation of IAPP in its natively amidated form at physiological pH in a membrane environment. Biochimica et Biophysica Acta (BBA) - Biomembranes. 2011; 1808:2337–2342. [PubMed: 21723249]
78. Knight JD, Hebda JA, Miranker AD. Conserved and cooperative assembly of membrane-bound α-helical states of islet amyloid polypeptide. Biochemistry. 2006; 45:9496–9508. [PubMed: 16878984]
79. Jha S, Snell JM, Sheftic SR, Patil SM, Daniels SB, Kolling FW, Alexandrescu AT. pH dependence of amylin fibrillization. Biochemistry. 2014; 53:300–310. [PubMed: 24377660]
80. Patil SM, Xu S, Sheftic SR, Alexandrescu AT. Dynamic alpha-helix structure of micelle-bound human amylin. J Biol Chem. 2009; 284:11982–11991. [PubMed: 19244249]
81. Khemtemourian L, Engel MF, Kruijtzer JA, Hoppener JW, Liskamp RM, Killian JA. The role of the disulfide bond in the interaction of islet amyloid polypeptide with membranes. Eur Biophys J. 2010; 39:1359–1364. [PubMed: 20052582]

82. Sciacca MF, Milardi D, Messina GM, Marletta G, Brender JR, Ramamoorthy A, La Rosa C. Cations as switches of amyloid-mediated membrane disruption mechanisms: calcium and IAPP. Biophys J. 2013; 104:173–184. [PubMed: 23332070]

83. Fadok VA, Bratton DL, Frasch SC, Warner ML, Henson PM. The role of phosphatidylserine in recognition of apoptotic cells by phagocytes. Cell Death Differ. 1998; 5:551–562. [PubMed: 10200509]

84. Van den Eijnde SM, Boshart L, Reutelingsperger CP, De Zeeuw CI, Vermeij-Keers C. Phosphatidylserine plasma membrane asymmetry in vivo: a pancellular phenomenon which alters during apoptosis. Cell Death Differ. 1997; 4:311–316. [PubMed: 16465246]

85. Koopman G, Reutelingsperger CP, Kuijten GA, Keehnen RM, Pals ST, van Oers MH. Annexin V for flow cytometric detection of phosphatidylserine expression on B cells undergoing apoptosis. Blood. 1994; 84:1415–1420. [PubMed: 8068938]

86. Ehses JA, Perren A, Eppler E, Ribaux P, Pospisilik JA, Maor-Cahn R, Gueripel X, Ellingsgaard H, Schneider MKJ, Biollaz G, Fontana A, Reinecke M, Homo-Delarche F, Donath MY. Increased number of islet-associated macrophages in type 2 diabetes. Diabetes. 2007; 56:2356–2370. [PubMed: 17579207]

87. Ehses JA, Boni-Schnetzler M, Faulenbach M, Donath MY. Macrophages, cytokines and beta-cell death in Type 2 diabetes. Biochemical Society Transactions. 2008; 36:340–342. [PubMed: 18481953]

88. Jourdan T, Godlewski G, Cinar R, Bertola A, Szanda G, Liu J, Tam J, Han T, Mukhopadhyay B, Skarulis MC, Ju C, Aouadi M, Czech MP, Kunos G. Activation of the Nlrp3 inflammasome in infiltrating macrophages by endocannabinoids mediates beta cell loss in type 2 diabetes. Nat Med. 2013; 19:1132–1140. [PubMed: 23955712]

89. Bakht O, Pathak P, London E. Effect of the structure of lipids favoring disordered domain formation on the stability of cholesterol-containing ordered domains (lipid rafts): identification of multiple raft-stabilization mechanisms. Biophys J. 2007; 93:4307–4318. [PubMed: 17766350]

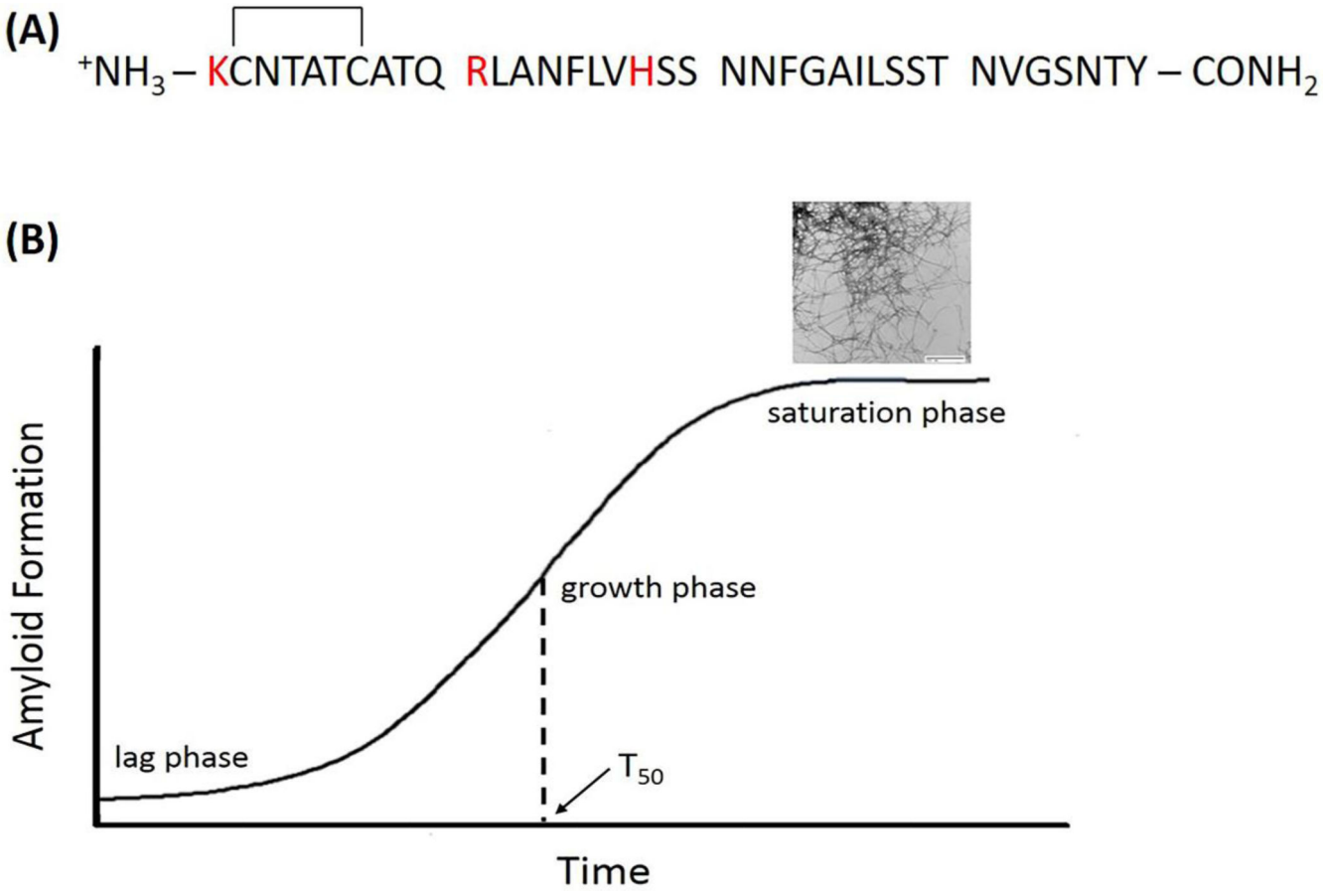

Figure 1.

(A) The sequence of hIAPP. The peptide has an amidated C-terminus and contains a disulfide bridge between residues 2 and 7. Residues which have the potential to be positively charged near physiological pH are colored red. **(B)** A schematic diagram of amyloid formation. The lag phase is followed by a growth phase which leads to a saturation phase. T_{50}, the time required to reach the midpoint of the lag phase is illustrated. The TEM image is of *in vitro* hIAPP amyloid fibrils.

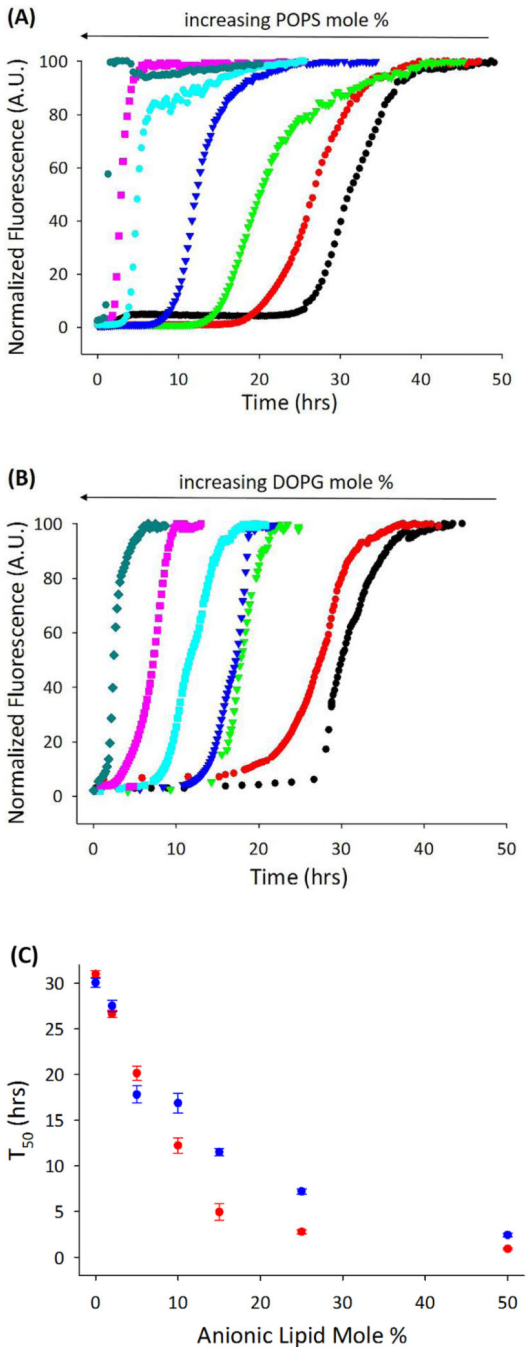

Figure 2. Anionic lipids increase the rate of amyloid formation

POPS and DOPG were separately mixed in vesicles with the zwitterionic lipid DOPC. The results of thioflavin-T experiments are displayed. **(A)** The effect of increasing the mole percent of POPS and **(B)** The effect of increasing the mole percent of DOPG. Data is plotted for anionic lipid concentrations of 50 mole percent (dark cyan); 25 mole percent (pink); 15 mole percent (cyan); 10 mole percent (blue); 5 mole percent (green); 2 mole percent (red); and 0 mole percent (black). **(C)** A plot of T_{50} vs the mole percent of anionic lipid: red,

POPS; blue, DOPG. Experiments were conducted in 20 mM Tris·HCl, 100 mM NaCl, pH 7.4 at 25 °C with 400 μM lipid and 20 μM hIAPP.

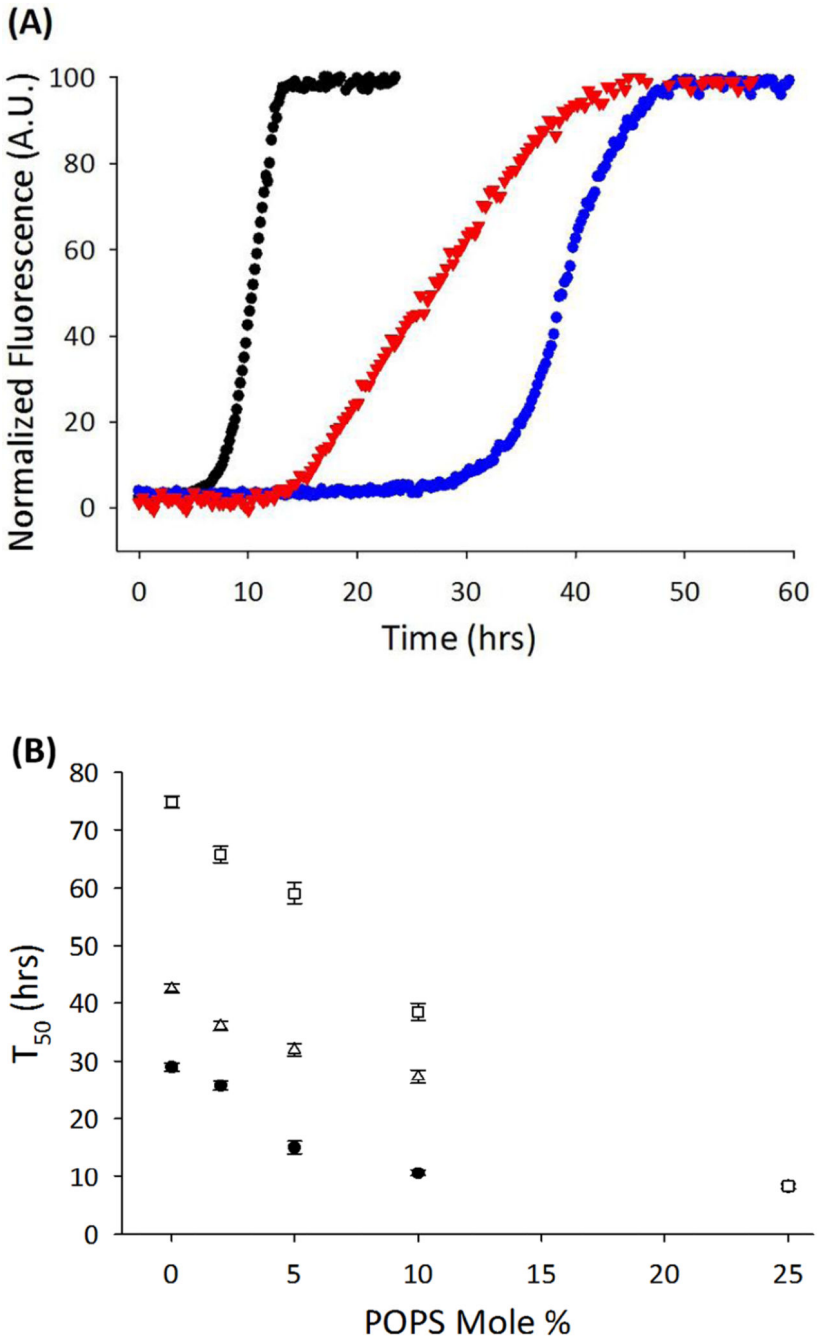

Figure 3. Cholesterol containing vesicles are less effective at promoting hIAPP amyloid formation

(A) Thioflavin-T assays for samples containing 10 mole percent POPS and different fractions of POPC and cholesterol are shown. Black, 10 mole percent POPS, 90 mole percent POPC; red, 10 mole percent POPS, 70 mole percent POPC, 20 mole percent cholesterol; blue, 10 mole percent POPS, 50 mole percent POPC, 40 mole percent cholesterol. **(B)** A comparison of the effects of 0, 20 and 40 mole percent of cholesterol on value of T_{50} using vesicles containing POPS and POPC as a function of POPS composition.

Solid circles, no cholesterol; open triangles, 20 mole percent cholesterol; open squares, 40 mole percent cholesterol. Experiments were conducted in 20 mM Tris·HCl, 100 mM NaCl, pH 7.4 buffer at 25 °C with 400 μM lipid and 20 μM hIAPP.

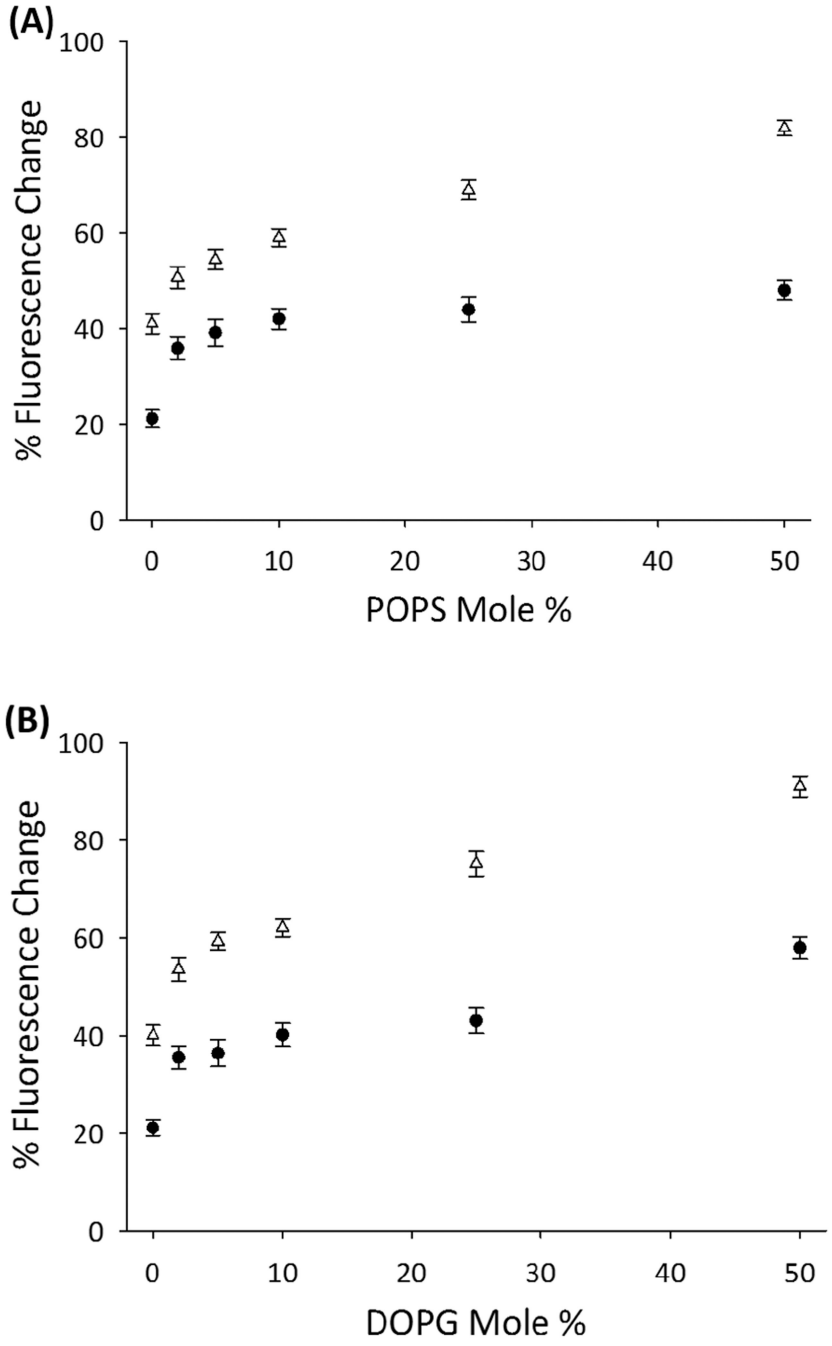

Figure 4. Analysis of the effect of POPS and DOPG on membrane leakage

The percentage change in 5(6)-carboxyfluorescein fluorescence is plotted vs the mole percent of anionic lipid. Leakage induced after 10 minutes (solid circles) and 40 hours (open triangles) of incubation with hIAPP is shown for vesicles that contain **(A)** DOPC and POPS and **(B)** DOPC and DOPG. Experiments were conducted in 20 mM Tris·HCl, 100 mM NaCl, pH 7.4 at 25 °C, 400 μM lipid, 20 μM hIAPP. hIAPP was added at time zero.

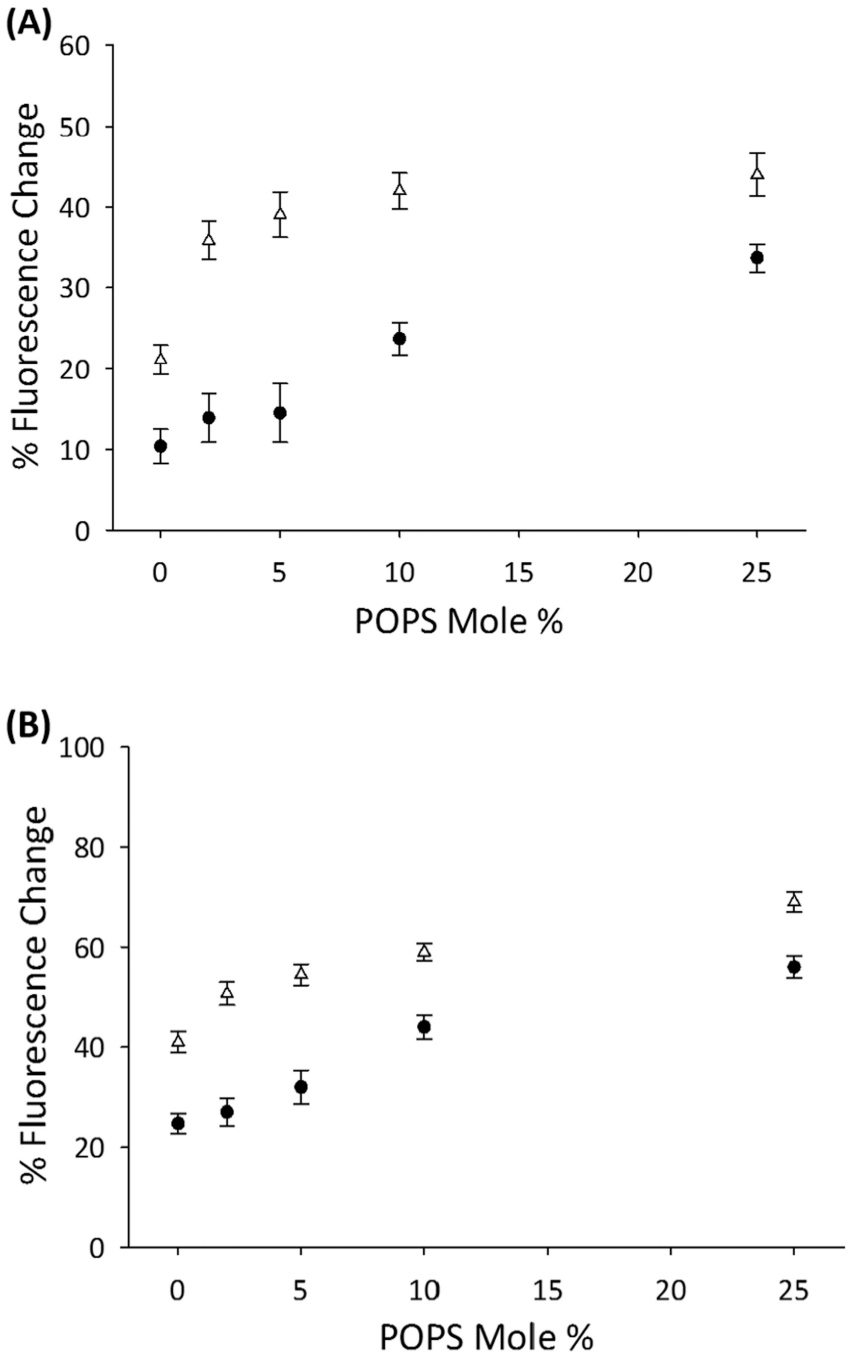

Figure 5. Comparison of the effect of DOPC and POPC on membrane leakage

The percentage change in 5(6)-carboxyfluorescein fluorescence is plotted vs the mole percent of POPS for vesicles that contain: solid circles, POPS and POPC; open triangles, POPS and DOPC. **(A)** Leakage induced after 10 minutes of incubation with hIAPP. **(B)** Leakage induced after 40 hours of incubation with hIAPP. Experiments were conducted in 20 mM Tris·HCl, 100 mM NaCl, pH 7.4 at 25 °C, 400 μM lipid, 20 μM hIAPP. hIAPP was added at time zero.

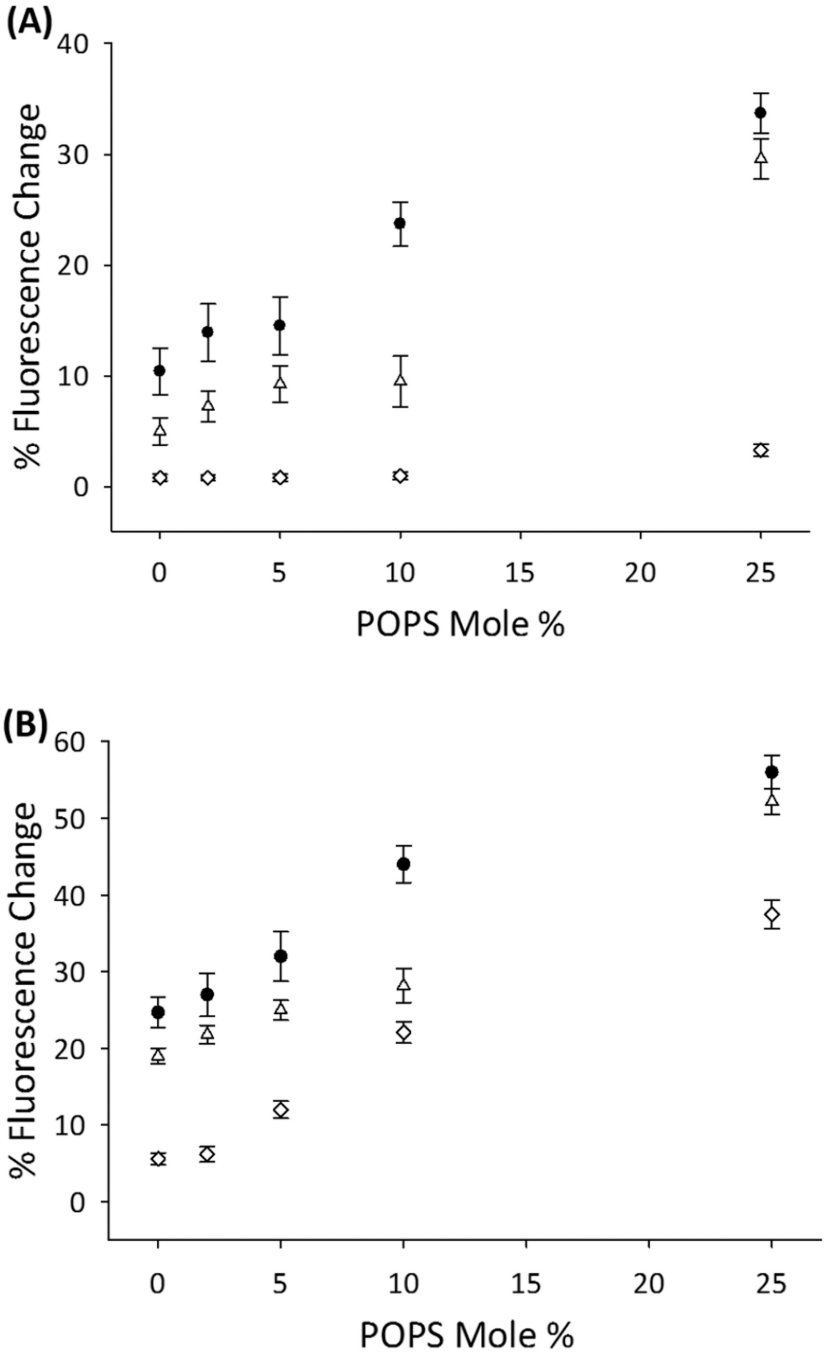

Figure 6. Analysis of the effect of cholesterol on membrane leakage

The percentage change in 5(6)-carboxyfluorescein fluorescence is plotted vs the mole percent of POPS. The effects of 0, 20 and 40 mole percent cholesterol on vesicles that contain POPS and POPC are compared. Solid circles, no added cholesterol; open triangles, 20 mole percent cholesterol; open squares, 40 mole percent cholesterol. **(A)** Leakage induced after 10 minutes of incubation with hIAPP. **(B)** Leakage induced after 120 hours of incubation with hIAPP. Experiments were conducted in 20 mM Tris·HCl, 100 mM NaCl, pH 7.4 at 25 °C, 400 μM lipid, 20 μM hIAPP. hIAPP was added at time zero.

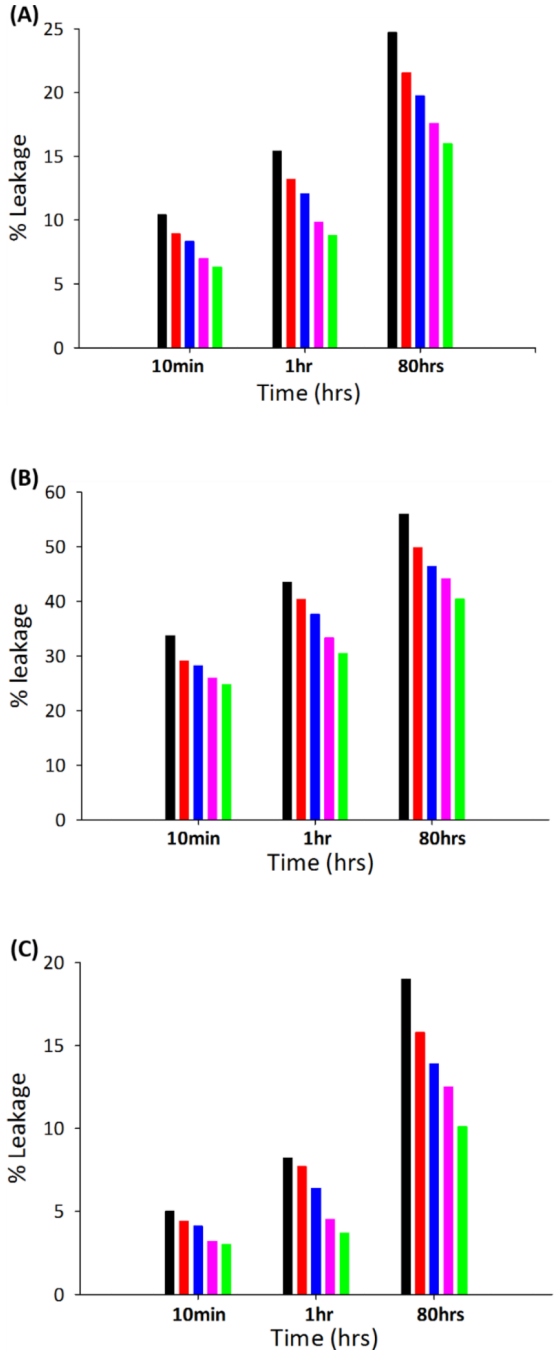

Figure 7. Membrane leakage of 5(6)-carboxyfluorescein (defined as percentage fluorescence change) and of different sizes of FITC-dextrans

The results of membrane leakage assays for 5(6)-carboxyfluorescein (black) and four FITC-dextrans of different sizes (red: 4100 Da; blue: 9400 Da; pink: 65600 Da; green: 154900 Da) are shown for: **(A)** 100 mole percent POPC **(B)** 75 mole percent POPC, 25 mole percent POPS and **(C)** 80 mole percent POPC, 20 mole percent cholesterol after incubation with hIAPP for 10 minutes, 1 hour and 80 hours. Experiments were conducted in 20 mM Tris·HCl, 100 mM NaCl, pH 7.4 at 25 °C with 400 μM lipid and 20 μM hIAPP.

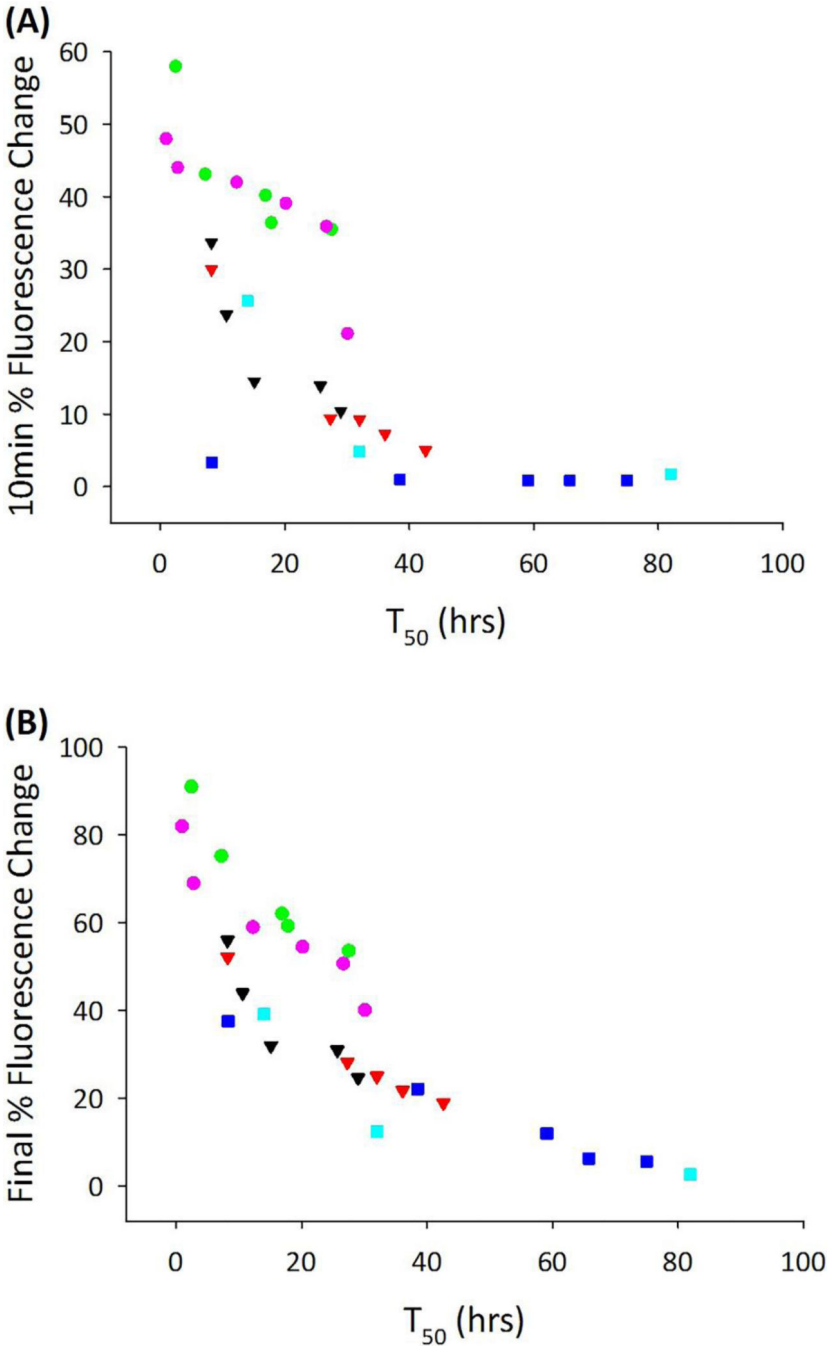

Figure 8. Correlation between the extent of leakage and the value of T_{50}

The percentage change in 5(6)-carboxyfluorescein fluorescence after **(A)** 10 minutes and **(B)** when amyloid formation is complete is plotted vs the value of T_{50} for all systems tested. Black: POPS(0–25 mole percent) + POPC; red: cholesterol(20 mole percent) + POPS(0–25 mole percent) + POPC; blue: cholesterol(40 mole percent) + POPS(0–25 mole percent) + POPC; green: DOPG(0–25 mole percent) + DOPC; pink: POPS(0–25 mole percent) + DOPC; cyan: 30 mole percent brain sphingomyelin + 60 mole percent POPC + 10 mole percent POPS; 50 mole percent brain sphingomyelin + 50 mole percent POPC; 30 mole

percent brain sphingomyelin + 30 mole percent POPC + 40 mole percent cholesterol. Experiments were conducted in 20 mM Tris·HCl, 100 mM NaCl, pH 7.4 at 25 °C with 400 μM lipid and 20 μM hIAPP.

Table 1

Summary of the values of T_{50} for amyloid formation, the percentage 5(6)-carboxyfluorescein fluorescence change observed after 10 minutes of incubation with hIAPP and the percentage 5(6)-carboxyfluorescein fluorescence change observed after samples were incubated long enough to reach the saturation phase of amyloid formation.

Composition of Membrane	T_{50} (hrs)	Percentage Fluorescence Change after 10min	Final Percentage Fluorescence Change
no membrane	41.8		
100% DOPC	30.1	21.1	40.1
2% DOPG + 98% DOPC	27.5	35.5	53.6
5% DOPG + 95% DOPC	17.8	36.4	59.3
10% DOPG + 90% DOPC	16.9	40.2	62.1
15% DOPG + 90% DOPC	11.5	ND	ND
25% DOPG + 75% DOPC	7.2	43.1	75.2
50% DOPG + 50% DOPC	2.4	58.0	91.0
2% POPS + 98% DOPC	26.7	35.9	50.7
5% POPS + 95% DOPC	20.2	39.1	54.5
10% POPS + 90% DOPC	12.2	42.0	59.0
15% POPS + 85% DOPC	5.0	ND	ND
25% POPS + 75% DOPC	2.8	44.0	69.0
50% POPS + 50% DOPC	0.9	48.0	82.0
100% POPC	29.0	10.4	24.7
2% POPS + 98% POPC	25.7	13.9	29.0
5% POPS + 95% POPC	15.1	14.5	32.0
10% POPS + 90% POPC	10.6	23.7	44.0
25% POPS + 75% POPC	8.2	33.7	56.0
80% POPC + 20% Chol	42.6	5.0	19.0
2% POPS + 78% POPC + 20% Chol	36.1	7.3	21.8
5% POPS + 75% POPC + 20% Chol	32.0	9.3	25.0
10% POPS + 70% POPC + 20% Chol	27.3	9.4	28.2
25% POPS + 55% POPC + 20% Chol	8.2	30.0	52.2
60% POPC + 40% Chol	75.0	0.8	5.6
2% POPS + 58% POPC + 40% Chol	65.8	0.8	6.2
5% POPS + 55% POPC + 40% Chol	59.1	0.8	12.0
10% POPS + 50% POPC + 40% Chol	38.5	1.0	22.1
25% POPS + 35% POPC + 40% Chol	8.3	3.3	37.5
30% BrSM + 30% POPC + 40% Chol	82.0	1.7	2.6
30% BrSM + 30% POPC + 40% Chol + 0.5% POPS	76.2	0.3	1.9
30% BrSM + 60% POPC + 10% POPS	14.0	25.6	39.2
50% BrSM + 50% POPC	32.0	4.9	12.4
50% EggSM + 50% POPC	38.0	4.1	15.0

Experiments were conducted in 20 mM Tris·HCl, 100 mM NaCl, pH 7.4 at 25 °C, 400 μM lipid, 20 μM hIAPP. BrSM = Brain sphingomyelin; EggSM = egg sphingomyelin; Chol = cholesterol; ND = not determined.

Table 2

Summary of the values of T_{50} for amyloid formation for different buffers.

Composition of Membrane	T_{50}(hrs)	Buffer
25% POPS + 75% POPC	1.5	20 mM Tris, no salt
25% POPS + 75% POPC	8.1	20 mM Tris, 100 mM NaCl
25% POPS + 75% POPC	4.0	20 mM phosphate, no salt
25% POPS + 75% POPC	6.5	20 mM phosphate, 100 mM NaCl
25% POPS + 75% POPC	1.4	10 mM phosphate, no salt

Experiments were conducted at 25 °C, with 400 μM lipid containing 25 mole percent POPS and 75 mole percent POPC, 20 μM hIAPP.